BJ Biomolecules

Biochem. J. (2014) **459**, 551–564 (Printed in Great Britain) doi:10.1042/BJ20131363

online data

Analysis of the co-operative interaction between the allosterically regulated proteins GK and GKRP using tryptophan fluorescence

Bogumil ZELENT*, Anne RAIMONDO†, Amy BARRETT†, Carol W. BUETTGER*, Pan CHEN*, Anna L. GLOYN† and Franz M. MATSCHINSKY*[1]

*Department of Biochemistry and Biophysics and Institute for Diabetes, Obesity and Metabolism, Perelman School of Medicine, University of Pennsylvania, Philadelphia, PA, U.S.A.
†Oxford Centre for Diabetes Endocrinology & Metabolism, University of Oxford, Oxford, U.K.

Hepatic glucose phosphorylation by GK (glucokinase) is regulated by GKRP (GK regulatory protein). GKRP forms a cytosolic complex with GK followed by nuclear import and storage, leading to inhibition of GK activity. This process is initiated by low glucose, but reversed nutritionally by high glucose and fructose or pharmacologically by GKAs (GK activators) and GKRPIs (GKRP inhibitors). To study the regulation of this process by glucose, fructose-phosphate esters and a GKA, we measured the TF (tryptophan fluorescence) of human WT (wild-type) and GKRP-P446L (a mutation associated with high serum triacylglycerol) in the presence of non-fluorescent GK with its tryptophan residues mutated. Titration of GKRP-WT by GK resulted in a sigmoidal increase in TF, suggesting co-operative PPIs (protein–protein interactions) perhaps due to the hysteretic nature of GK. The affinity of GK for GKRP was decreased and binding co-operativity increased by glucose, fructose 1-phosphate and GKA, reflecting disruption of the GK–GKRP complex. Similar studies with GKRP-P446L showed significantly different results compared with GKRP-WT, suggesting impairment of complex formation and nuclear storage. The results of the present TF-based biophysical analysis of PPIs between GK and GKRP suggest that hepatic glucose metabolism is regulated by a metabolite-sensitive drug-responsive co-operative molecular switch, involving complex formation between these two allosterically regulated proteins.

Key words: allosteric regulation, co-operativity, diabetes, fructose phosphate ester, glucokinase, glucokinase regulatory protein, metabolic regulation.

INTRODUCTION

The hexokinase GK (glucokinase) plays a critical role in the regulation of hepatic glucose metabolism [1–4]. It has a relatively low affinity for glucose (approximately 7.5 mM), allowing it to adjust its activity precisely in response to physiological changes in blood and intrahepatic glucose concentrations. This enables effective clearance of glucose from the blood after a meal. In contrast with other hexokinases, GK displays a sigmoidal activity curve with regard to glucose and is not inhibited by its product, glucose 6-phosphate, or other metabolites [4,5]. Approximately 99.9 % of the body's entire supply of GK resides in the liver, with the remainder expressed in the endocrine cells of the pancreas, enteroendocrine cells, pituitary gonadotropes and selected nuclei of the central nervous system [3].

Gene expression and post-translational regulation of GK are profoundly influenced by its location in the body. In the liver its expression is effectively controlled by insulin such that absence of this hormone results in near total loss of GK expression within a few days [1,2,6–9]. Its enzymatic activity is also regulated within minutes by binding of the liver-specific regulatory protein GKRP (GK regulatory protein) [6–9]. GKRP is present in liver cells in a 2–3-fold molar excess compared with GK, and its expression is relatively independent of food intake and hormonal status. In complexing with GK, GKRP performs at least two functions: first, it serves as a cytosolic chaperone, allowing entry of GK into the nuclear space via the NPC (nuclear pore complex) [10,11]; and secondly, it creates an inactive nuclear pool of GK that can be readily released in response to changes in hepatic glucose or fructose levels. [1,2,6–11]. Cytosolic GK–GKRP protein complex assembly and nuclear trafficking are also modulated by phosphorylated hexose metabolites. Glucose and F1P (fructose 1-phosphate), a product of fructose and sorbitol metabolism, oppose GK–GKRP complex formation, nuclear sequestration and subsequent inhibition of GK activity, whereas F6P (fructose 6-phosphate), an intermediate of glycolysis, glycogenolysis and gluconeogenesis, counters these actions, at least in humans [12,13]. GKAs (GK activators) [3,14–21] and GKRPIs (GKRP inhibitors) [22], novel classes of drugs with potential as anti-diabetic agents, also disrupt the GK–GKRP complex, thus enhancing hepatic glucose uptake [3,19–22]. The exit of free GK from the nucleus is independent of GKRP and is mediated by the enzyme's nuclear export signal [10,11].

To understand these complex liver-specific regulatory mechanisms, it is necessary to account, at least semi-quantitatively, for the participating cellular compartments, i.e. the cytosolic and nuclear spaces. The relative nuclear volume of the hepatocyte is approximately 5 % in the fed state, and may increase to 10–15 % after extended starvation [1,23,24]. The distribution of GK between these two compartments is known to differ markedly in the fed compared with the fasting state; it is primarily cytosolic in the former and primarily nuclear in the latter [1,8–11]. In contrast, GKRP resides almost exclusively in the nuclear space. In fact, it is difficult to detect GKRP in the cytosol via routine

Abbreviations: F1P, fructose 1-phosphate; F6P, fructose 6-phosphate; GCK/GK, glucokinase; GCKR/GKRP, GK regulatory protein; GKA, GK activator; GKRPI, GKRP inhibitor; hGK, human GK; hGKRP, human GKRP; MH, D-mannoheptulose; NATA, *N*-acetyl-L-tryptophanamide; NPC, nuclear pore complex; PPI, protein–protein interaction; rGKRP, rat GKRP; SIS, sugar isomerase; T2D, Type 2 diabetes; TF, tryptophan fluorescence; WT, wild-type; xGK, *Xenopus* GK; xGKRP, *Xenopus* GKRP.

[1] To whom correspondence should be addressed (email matsch@mail.med.upenn.edu).

histochemical methods, regardless of nutritional status. Model calculations based on an assumed increase in relative nuclear volume during fasting from 5 % to 10 % or even 15 % [1,23,24], illustrate that the cytosolic and nuclear concentrations and ratios of these two interacting proteins undergo dramatic changes during regular or imposed feeding–fasting cycles. For example, assuming an equal concentration of GK in the two compartments in the fed state, the total cytosolic amount of free active enzyme would be approximately 20-fold higher that in the nucleus, and the GK/GKRP ratio would probably be high, approaching a factor of 5–10. Alternatively, assuming 66 % nuclear sequestration of total GK during fasting would result in a 10–20-fold increase in the nuclear concentration of GK and a subsequent increase in the nuclear GK/GKRP ratio from approximately 1:50 to approximately 1:4, still guaranteeing near complete inhibition of nuclear GK activity by GKRP. These considerations have implications for our understanding of the GK–GKRP interaction, and are taken into account in the design of the present investigation (see below).

The critical role of GK and its regulation by GKRP are illustrated by the impact that genetic variation in the genes that encode these proteins have on normal glucose and triacylglycerol metabolism in humans [25–32]. Over 600 naturally occurring mutations in the *GCK* (glucokinase) gene have been described, which have a wide range of functional consequences including inactivation or activation of catalytic capacity, structural and functional protein instability and decreased responsiveness to GKRP [29]. Heterozygous inactivating *GCK* mutations cause an autosomal dominantly inherited condition characterized by mild fasting hyperglycaemia, whereas inheritance of two defective *GCK* alleles results in the more severe phenotype of permanent neonatal diabetes [25,27]. In contrast, heterozygous activating mutations cause the opposite phenotype of hypoglycaemia, whereas homozygous cases have not been found because they are probably lethal [26]. A common non-synonymous variant (P466L) in *GCKR*, the gene that encodes GKRP, present in the healthy population has been reproducibly associated with fasting serum triacylglycerol and glucose levels [33]. Functional characterization of this variant protein has demonstrated that it is a less effective inhibitor of GK and results in reduced nuclear storage of GK [28,31]. Moreover, rare variants in *GCKR* have been shown to be associated with serum triacylglycerol and cholesterol levels in healthy adults and to be overrepresented in individuals with hypertriglyceridaemia (Figure 1C) [30,32].

In light of the central role of the GK–GKRP complex in glucose homoeostasis and its subsequent causal involvement in the pathogenesis of T2D (Type 2 diabetes), hypoglycaemia and hypertriglyceridaemia, it is not surprising that intensive efforts have been directed towards developing pharmacological agents that target both proteins [3,14–16,18–21,22,34]. These efforts have resulted in the discovery of GKAs a decade ago [15] and of GKRPIs in 2013 [22], which have an as yet unrealized potential as anti-diabetic agents. These pharmacological agents are of interest to the present investigation because of their capacity to disrupt the GK–GKRP complex, thereby indirectly enhancing glucose uptake and glycogen synthesis and also, potentially, lipid biosynthesis via GK activation.

Since the discovery of the GK and GKRP proteins, our understanding of the structural and functional biophysics of GK and GKRP and the manner in which they interact has steadily been advanced [1–7,9,35–46]. Kinetic, crystallographic and NMR studies have demonstrated that GK displays co-operative kinetics with respect to glucose (as indicated by a Hill coefficient of approximately 1.7), operates as a monomer, and exhibits a continual oscillation between low and high affinity conformations at a rate that is lower than that of the catalytic cycle, commonly referred to as hysteresis [36,44–46]. Biophysical characterization of GKRP and its interaction with GK has developed more slowly [9,19–21], but has recently benefited from the publication of several landmark crystallographic studies that provide detailed structural information about this protein and its PPIs (protein–protein interactions) with GK (Figures 1A and 1B) [22,47–49]. GKRP (of human, rat and frog origin alike) was shown to be a monomer, with a trilobate structure resembling the structure of SISs (sugar isomerases), featuring deeply buried allosteric sites: one for fructose-phosphate esters [47–49] and the other for GKRPIs [22]. There is clear evidence for conformational changes within GKRP (as shown for the rat protein) upon the allosteric binding of fructose-phosphate esters qualitatively distinguishing between the effects of F1P and F6P [49]. Choi et al. [47] succeeded in crystallizing and characterizing the *Xenopus laevis* GK–GKRP complex. One should remember here that xGKRP (*Xenopus* GKRP) is functionally unresponsive to fructose-phosphate esters, apparently the result of a critical H350P substitution. Beck and Miller [49] crystallized and characterized a GK–GKRP complex of rat GKRP and human pancreatic GK showing the same structural features as observed for the complex of frog proteins. The crystallographic observations of Choi et al. [47] and of Beck and Miller [49] thus demonstrate that the common GKRP-binding site on GK is located within the flexible hinge region which links the smaller and larger lobes of the enzyme. In combination with mutational analyses of hGKRP (human GKRP) and GKA binding to hGK (human GK) using TF (tryptophan fluorescence) or enzyme kinetics [21], these studies provide compelling evidence that GKRP and GKA bind to spatially distinct receptors in the allosteric modifier region of GK.

Notwithstanding this significant body of established knowledge, it remains to be clarified exactly how the complex system regulating hepatic glucose phosphorylation operates during feeding–fasting cycles, in pathological states, including T2D and hypoglycaemia, and in response to pharmacological intervention. As discussed above, highly effective allosteric and co-operative mechanisms coupled with intricate compartmental controls have evolved to regulate this process. In the present investigation, we used TF as a means to study hGK–hGKRP complex assembly and disassembly [37,39,41,43,50,51]. GKRP has six highly conserved tryptophan residues at positions Trp^{19}, Trp^{222}, Trp^{335}, Trp^{461}, Trp^{484} and Trp^{517} [48,49], randomly distributed throughout its trilobate structure (Figure 1). We used both GK-WT and a non-fluorescent form of GK in which its three native tryptophan residues were mutated (GK-W99R/W167F/W257F) to explore the interaction between GK and hGKRP-WT and GKRP-P446L, using the average TF of GKRP as an indicator of its conformation in its free and bound forms [51].

MATERIALS AND METHODS

Commercial materials and preparation of recombinant proteins

NATA (*N*-acetyl-L-tryptophanamide), D-glucose and D-fructose 6-phosphate disodium salt were supplied by Sigma Chemical. D-fructose 1-phosphate sodium salt was supplied by Santa Cruz Biotechnology. The non-fluorescent GKA used in the present study was RO0274375-000 [21,50,51]. Generation of GST-tagged islet GCK-WT, FLAG-tagged WT (wild-type) and GCKR-P446L bacterial expression vectors has been described previously [28,52]. Point mutations were introduced into the GST-GCK vector using the QuikChange II site-directed mutagenesis kit

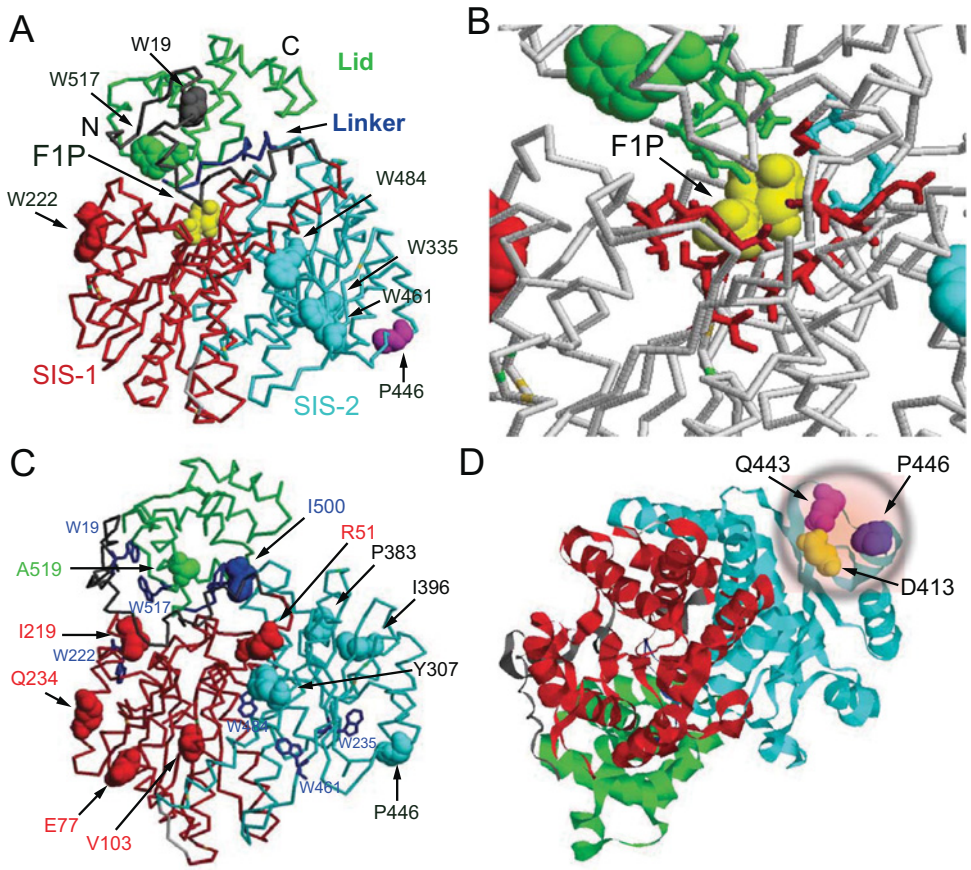

Figure 1 Structure of GKRP

(**A**) Locations of tryptophan residues in GKRP domains: Trp^{19} at the N-terminus (6–44; grey), Trp^{222} in the SIS-1 domain (45–284; red), Trp^{335}, Trp^{461} and Trp^{483} in the SIS-2 domain (289–499; cyan), and Trp^{517} in the Lid (513–606; green). The linker between SIS-1 and the Lid is shown in blue. The P446L point mutation is shown in magenta. F1P bound to one of the two known allosteric sites is shown in yellow. The second allosteric site for GKRPIs, situated between the Lid and the SIS-1–SIS-2 complex [22] is not shown. (**B**) Magnified view of the fructose phosphate-binding site to indicate the amino acids involved in F1P and F6P binding: Asn^{512}, Lys^{514}, Leu^{515} and Arg^{518} in the Lid (green), Glu^{348} and His^{351} in the SIS-2 domain (cyan), and Gly^{107}, Thr^{109}, Ser^{110}, Glu^{153}, Leu^{178}, Ser^{179}, Val^{180}, Gly^{181}, Leu^{182}, Ser^{183}, Gly^{256}, Ser^{258} and Arg^{259} in the SIS-1 domain (red) (PDB code 4BB9). (**C**) The widely dispersed location of functional variants associated with triacylglycerol levels in GKRP. (**D**) The close proximity of the common mutant P446L to Asp^{413} [47] and Gln^{443} [49] forming a critical salt bridge to Arg^{186} of GK is illustrated.

according to the manufacturer's instructions (Stratagene). The tryptophan residue-free GK made for the present study was GK-W99R/W167F/W257F. All mutant constructs were verified by DNA sequencing. Recombinant human β-cell GK was subsequently expressed in *Escherichia coli* cells and purified as described previously [52,53]. The GST-fusion proteins were then cleaved with factor Xa and submitted to a second round of purification using Benzamidine Sepharose 6B (GE Healthcare) according to the manufacturer's instructions. Recombinant GK-W99R/W167F/W257F protein was expressed in significant amounts and was found to be essentially pure as indicated by the presence of a single band at 50 kDa via gel chromatography (results not shown). Recombinant human GKRP-WT and GKRP-P446L were also expressed in *E. coli* cells and purified to homogeneity as described previously [28].

Absorption and fluorescence measurements

UV–visible absorption

Spectra were measured using a Hitachi PerkinElmer U-3000 spectrophotometer.

Fluorescence

Spectra were measured with a Fluorolog-3-21 Jobin-Yvon Spex Instrument SA equipped with a 450 W Xenon lamp for excitation and a cooled R2658P Hamamatsu photomultiplier tube for detection. For all measurements, 90° geometry was employed and 295 nm excitation wavelengths were used to observe fluorescence emission in the 300–500 nm range. For TF, spectra slit width was set to provide a bandpath of 3 nm for excitation and 3 nm for emission. Spectra were corrected for instrumental response using Spex instrument software. A thermostatically controlled cell holder maintained sample temperature at 20 °C. A thermocoupler was used to measure sample temperature. The buffer used contained 20 mM phosphate, 50 mM KCl, 1 mM EDTA and 1 mM DTT (pH 7.2).

Quantum yields

Fluorescence quantum yields of tryptophan (Φ) were determined for GKRP-WT and GKRP-P446L using eqn (1) [54]:

$$\Phi_S = \Phi_R \, (A_R/A_S) \, (F_S/F_R) \, (n_S^2/n_R^2) \quad (1)$$

where S and R refer to sample and reference standard respectively, A_R and A_S denote absorbance at the excitation wavelength, F_S and F_R denote the integral intensities of the recorded fluorescence spectra measured under identical instrument settings, and n_S and n_R are the refractive indices. Fluorescence quantum yields were determined relative to NATA ($\Phi = 0.14$) [55].

Titration curves for binding of GK-W99R/W167F/W257F to GKRP-WT or GKRP-P446L

Fluorescence data were obtained via the stepwise addition of the appropriate amount of non-fluorescent GK-W99R/W167F/W257F to GKRP in a fluorescence cuvette. TF spectra were measured for GKRP in the presence of increasing amounts of GK-W99R/W167F/W257F, and spectra intensities corrected according to the background fluorescence of GK-W99R/W167F/W257F alone under the same experimental conditions. The change in GKRP protein fluorescence during titration was also measured using time-dependent scans. A manual procedure was used such that a typical titration with 10–12 additions required 20–25 min to perform. The same buffer as described above was routinely used unless stated otherwise. The bandpath was 0.5 nm at 295 nm for excitation and 12 nm at 340 nm for emission. Data were corrected for experimental dilution and then fit to the Langmuir saturation function $F = \{F_0 + (F_{sat} - F_0)\}\{[x]^H/([x]^H + K_D{}^H)\}$, also known as the Hill equation, where H is the Hill number and x was F6P, F1P, GK-W99R/W167F/W257F, GKA or D-glucose. For some graphical presentations the linear form of the Hill equation was used: $\log[F/(F_{sat} - F)] = H \log x - H \log K_D$ [46].

Protein concentration

The molar concentration of proteins was determined from UV absorption measurements in a quartz cuvette using a pathlength of 1 cm and a molar absorption coefficient at 280 nm of 47 900 $M^{-1} \cdot cm^{-1}$ for GKRP-WT [19] and 18 510 $M^{-1} \cdot cm^{-1}$ for GK-W99R/W167F/W257F, which was calculated based on previously established values for GK-WT (35 130 $M^{-1} \cdot cm^{-1}$) [35] and tryptophan (5540 $M^{-1} \cdot cm^{-1}$) [56].

The kinetics of ligand-induced slow conformational transitions of GK

Kinetic traces were monitored by TF in a quartz cuvette using 295 ± 0.5 nm for excitation and 340 ± 5 nm for emission at a temperature range of 5–25 °C. These slow transitions were initiated by adding MH (D-mannoheptulose) to a final concentration of 5 or 10 mM to an assay mixture containing $\sim$1 μM GK and 20 μM GKA. MH is a competitive inhibitor of GK and was used because the TF transitions in its presence are slower than those observed with glucose, thus facilitating kinetic analyses. For GK-W99R/W257F, the activation process was initiated by adding GKA in the absence of MH. The temperature dependence of the fluorescence tracings (see Supplementary Figure S1 at http://www.biochemj.org/bj/459/bj4590551add.htm) was fitted and analysed using the Risefall exponential model [57]. From the Arrhenius relationship $\ln k = \ln A - E_a/RT$, and based on the precepts of transition state theory [58], we obtained the activation energy (E_a) and other thermodynamic parameters of ligand-induced GK activation: enthalpy (ΔH°; kJ/mol), entropy (ΔS°; kJ/molK) and free energy of activation (ΔG°; kJ/mol), which were expressed as $\Delta H^\circ = E_a - RT$, $\Delta S^\circ = R[\ln A - 1 - \ln(k_B T/h)]$ and $\Delta G^\circ = \Delta H^\circ - T\Delta S^\circ$ respectively, where k_B is the Boltzman constant, h is the Planck constant, R the gas constant and T the absolute temperature. Kinetic data of the transition and thermodynamic parameters for WT and mutant GK are recorded in Supplementary Table S1 (http://www.biochemj.org/bj/459/bj4590551add.htm).

Precision estimates

The numerical values of all Tables are the results of individual experiments. In many, but not all, instances results were verified by additional measurements. This approach is state of the art for studies of the present type, but was also dictated by the scarcity of the recombinant proteins combined with the strategy of using a large variety of experimental conditions to explore GK–GKRP interaction in depth.

Graphics

Structural considerations for GKRP are based on PDB code 4BB9 [48] and 4LC9 [49] and for GK on PDB codes 1V4T (open form) and 1V4S (closed form) [38] using the RasMol program (version 2.7.1).

RESULTS AND DISCUSSION

Conceptual and methodological considerations

This investigation is based on a conceptual model of the GK–GKRP interaction, which was first suggested by Shiota et al. [11] and Bosco et al. [10] and subsequently reviewed by Agius [1] and Iynedjian [2]. This model proposes that GKRP plays a dual role in the regulation of GK. First, it behaves as a chaperone for GK transfer into the nucleus, as GK itself appears to lack a functional NLS (nuclear localization signal). Secondly, GKRP retains GK in the nucleus in an inactive, but readily accessible, inhibitory complex. The critical step in GK–GKRP complex formation is investigated in the present paper biophysically by TF under conditions mimicking the cytosol, at GK/GKRP ratios ranging from 1:1 to 10:1. These TF studies were performed at micromolar protein concentrations similar to those that occur in the cytosol. Complex formation was monitored via detection of changes in GKRP TF in the presence of increasing amounts of non-fluorescent GK-W99R/W167F/W257F. The common disease-associated variant protein GKRP-P446L, which has been well characterized in biochemical, genetic and cell biological studies [28,30,31], was also used to explore the potential of these TF-based methods of analysis and provided the means to assess the contribution of structural instability and/or impaired protein folding to the effectiveness of GKRP as a GK regulator [50]. Further critical experimental material and conceptual commentary on the biochemical characteristics of GK-W99R/W167F/W257F are shown in the Supplementary Online Data to facilitate the interpretation of the present model studies on GK–GKRP interactions employing this non-fluorescent reagent (Supplementary Figures S1–S4 and Tables S1–S3 with associated text and discussion at http://www.biochemj.org/bj/459/bj4590551add.htm). This Supplementary Online Data shows that the modified GK molecule retains its unique biochemical features with one exception: the activation of GK-W99R/W167F/W257F by GKAs is rendered glucose-independent as a result of the Trp^{99} substitution by arginine which makes the allosteric drug receptor site of the enzyme freely accessible to GKAs.

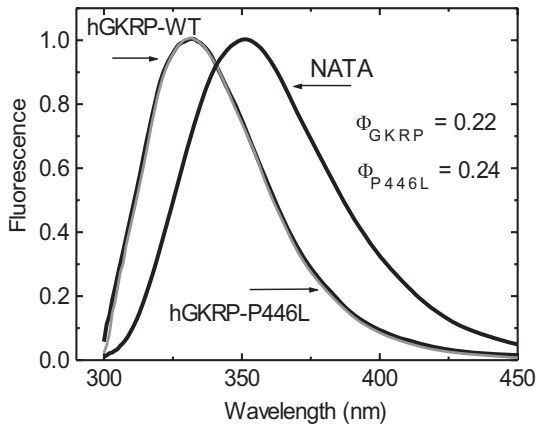

Figure 2 Normalized TF spectra for 0.3 μM GKRP-WT and GKRP-P446L compared with tryptophan–NATA (λ_{exc} = 295 nm)

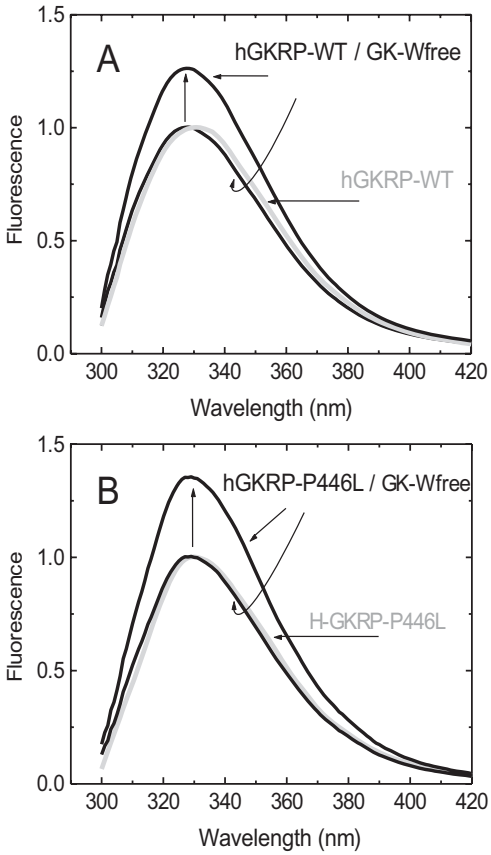

Figure 3 TF spectra for 0.3 μM GKRP in the presence or absence of 5 μM GK at 20 °C showing the fluorescence increase (vertical arrows) and blue shift of the spectra upon GK binding for GKRP-WT (A) and GKRP-P446L (B) (λ_{exc} = 295 nm)

GK-Wfree, GK-W99R/W167F/W257F.

Assessment of the basic TF characteristics of recombinant hGKRP

The high average quantum yield of GKRP TF allowed for accurate measurements at 0.3 μM GKRP-WT and GKRP-P446L. The two proteins showed comparable spectra and quantum yields with the same TF maxima at 332 nm (Figures 2 and 3, and Supplementary Table S4 at http://www.biochemj.org/bj/459/bj4590551add.htm). Saturating amounts of GK (5 μM) increased the TF of GKRP-WT by 29 % and GKRP-P446L by 44 % (Figure 3 and Table 1). GK addition also caused a comparable blue shift in the TF maxima by 3–5 nm (Figure 3, and Supplementary Figures S5 and S6 at http://www.biochemj.org/bj/459/bj4590551add.htm). These results imply that GKRP undergoes a conformational change during complex assembly, which has been previously observed for the hGK–rGKRP (rat GKRP) complex crystallographically [49] and for the hGK–hGKRP complex by MD [47], but not with xGK (*Xenopus* GK) and xGKRP by crystallography [47]. Glucose, F6P, F1P and GKA had differential effects on the TF of GKRP-WT and GKRP-P446L. Glucose had no effect on the fluorescence of GKRP-WT, but lowered the TF signal observed for GKRP-P446L, suggesting that this amino acid substitution modifies the sugar phosphate-binding site of GKRP in a manner that specifically affects binding of unphosphorylated hexoses (Supplementary Figures S7 and S8 at http://www.biochemj.org/bj/459/bj4590551add.htm). An increase and decrease in the TF signal for both GKRP-WT and GKRP-P446L was observed in the presence of F6P and F1P respectively. Remarkably, positive as well as negative ΔTF values for GKRP-P446L were twice that of WT-GKRP for both phosphate esters (Table 1). Also noteworthy is the sigmoidal shape of the TF concentration-dependency curve for F6P contrasting with the hyperbolic shape of that for F1P as indicated by the different Hill coefficients. A corollary for these opposite effects of the two fructose-phosphate esters on GKRP TF are crystallographic observations showing that the Lid domain/SIS-2 interface of GKRP is differentially affected by the two ligands [49]. The TF changes encountered in the present study ranged in magnitude from 4 to 44 % and therefore allowed for accurate ligand concentration-dependency studies, as well as assessment of the structural stability and refolding capacity of GKRP-WT and GKRP-P446L following denaturation by urea.

Assessment of structural stability and studies of unfolding/refolding cycles of GKRP-WT and GKRP-P446L

A measure of the structural stability of GKRP-WT and GKRP-P446L, as well as the ability of these two proteins to refold spontaneously upon denaturation, were critical for the biophysical studies described in the present paper [50,59]. We found that GKRP-WT is a relatively labile protein, as indicated by a $\Delta G(H_2O)$ of 1.56 kcal/mol, and is comparable with GK-WT (1.63 kcal/mol). Both GKRP-WT and GK-WT refold readily upon denaturation with 8 M urea (Figure 4 and Supplementary Table S5 at http://www.biochemj.org/bj/459/bj4590551add.htm). Furthermore, GKRP-WT and GKRP-P446L displayed comparable $\Delta G(H_2O)$ of denaturation (1.56 and 1.55 kcal/mol respectively) and unfolding/refolding patterns, suggesting that structural instability is unlikely to explain the metabolic effects of this variant protein. This conclusion is strengthened by results obtained by comparison with the proven instability mutants GK-M298K and GK-S263P [59] which clearly showed a lowering of their ΔG of denaturation and impaired refolding after urea denaturation (Figure 4 and Supplementary Table S5).

Demonstrating co-operativity in the assembly of the GK–GKRP complex

In order to mimic the concentrations of GK and GKRP likely to occur in the cytosol, assembly of these two proteins

Table 1 GKRP-WT or GKRP-P446L interaction in the absence and presence of GK-W99R/W167F/W257F, F6P, F1P, D-glucose and GKA at 20°C measured by the TF of GKRP

ΔF is the relative fluorescence change at 340 nm.

GKRP	Additional agents	ΔF	$S_{0.5}$ (μM)	H
GKRP-WT	F6P	0.04	278	3.6
GKRP-P446L	F6P	0.07	242	2.94
GKRP-WT	F1P	− 0.04	65	1
GKRP-P446L	F1P	− 0.08	139	1
GKRP-WT	D-Glucose	0	–	–
GKRP-P446L	D-Glucose	− 0.06	27 mM	1.49
GKRP-WT	GK-W99R/W167F/W257F	0.29	1.22	1.74
GKRP-P446L	GK-W99R/W167F/W257F	0.44	2.05	1.86
GKRP-WT	F6P and GK-W99R/W167F/W257F	0.31	1.20	1.71
GKRP-P446L	F6P and GK-W99R/W167F/W257F	0.44	1.66	1.31
GKRP-WT	F1P and GK-W99R/W167F/W257F	0.32	2.68	2.8
GKRP-P446L	F1P and GK-W99R/W167F/W257F	0.41	2.95	2.84
GKRP-WT	D-Glucose and GK-W99R/W167F/W257F	0.42	2.56	2.78
GKRP-P446L	D-Glucose and GK-W99R/W167F/W257F	0.43	3.38	2.94
GKRP-WT	GKA and GK-W99R/W167F/W257F	0.42	2.77	3.4
GKRP-P446L	GKA and GK-W99R/W167F/W257F	0.43	2.59	2.17
GKRP-WT	D-Glucose, F6P and GK-W99R/W167F/W257F	0.35	2.43	2.83
GKRP-P446L	D-Glucose, F6P and GK-W99R/W167F/W257F	0.42	2.84	2.45
GKRP-WT	D-Glucose, F1P and GK-W99R/W167F/W257F	0.33	3.3	2.25
GKRP-P446L	D-Glucose, F1P and GK-W99R/W167F/W257F	0.44	2.97	2.77
GKRP-WT	D-Glucose, GKA and GK-W99R/W167F/W257F	0.42	4.75	3.2
GKRP-P446L	D-Glucose, GKA and GK-W99R/W167F/W257F	0.42	3.55	2.68

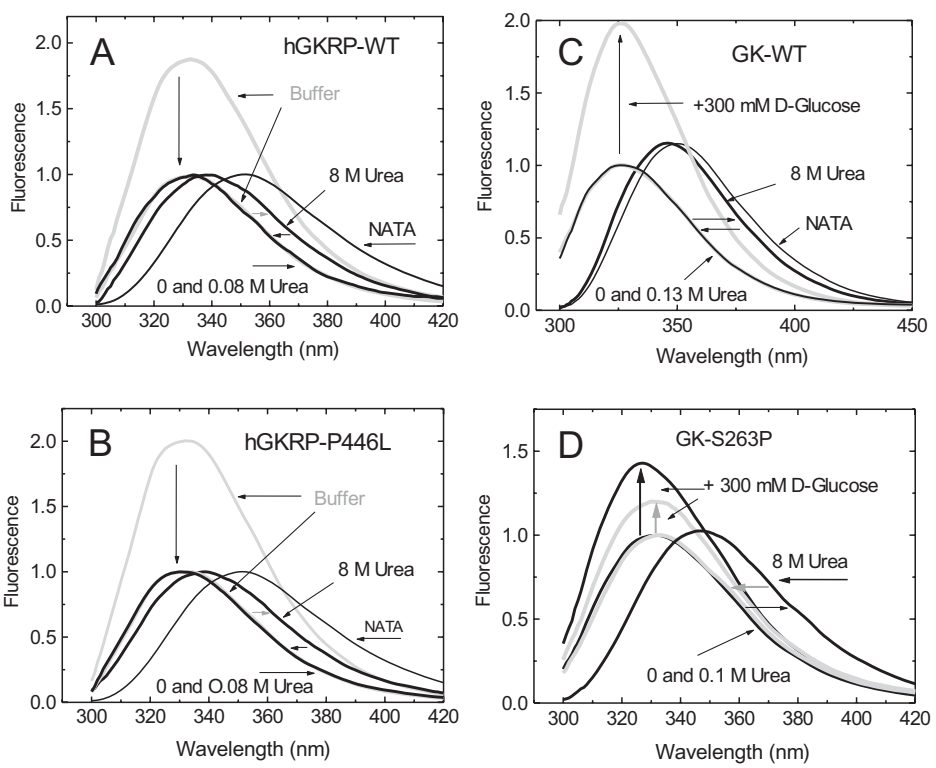

Figure 4 Structural stability and unfolding/refolding cycles of GKRP-WT and GKRP-P446L

TF spectra for 0.3 μM GKRP in the presence or absence of 8 M urea at 20°C for GKRP-WT (**A**) and for GKRP-P446L (**B**). The horizontal arrows show the red and blue shifts of the spectra during denaturation and refolding at 4°C respectively. Vertical arrows show the TF spectra of the proteins in buffer normalized to 1. (**C**) TF spectra of WT-GK and (**D**) established instability mutant GK-S263P in the presence or absence of 8 M urea ($\lambda_{exc} = 295$ nm).

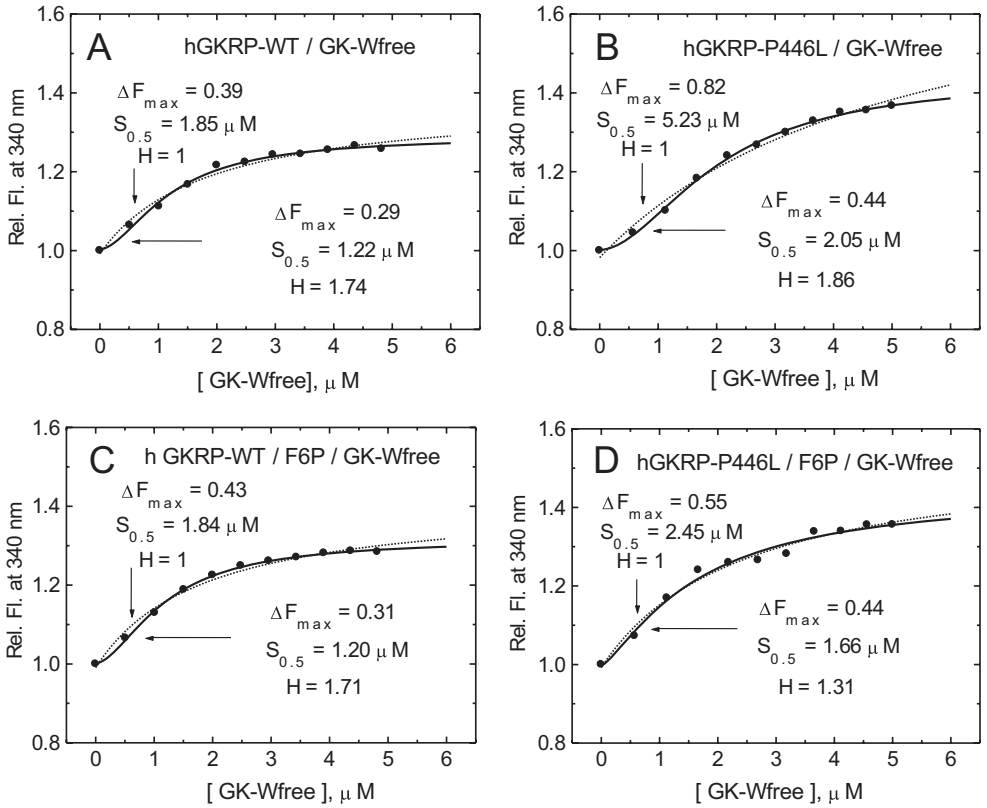

Figure 5 Co-operativity of GK–GKRP complex assembly

(**A** and **B**) Relative TF increase for 0.3 μM GKRP in the presence of increasing amounts of GK-W99R/W167F/W257F (GK-Wfree) for GKRP-WT (**A**) and for GKRP-P446L (**B**). (**C** and **D**) The effect of increasing amounts of GK-W99R/W167F/W257F on the TF of 0.3 μM GKRP in the presence of 500 μM F6P are shown for GKRP-WT (**C**) and GKRP-P446L (**D**) ($\lambda_{exc} = 295$ nm; $\lambda_{em} = 340$ nm). Comparison of the curve fitting by simple saturation or sigmoidal functions is shown in Supplementary Table S6 (at http://www.biochemj.org/bj/459/bj4590551add.htm).

was studied at a constant GKRP concentration of 0.3 μM with increasing amounts of GK ranging from 0.5 to 5 μM. Sigmoidal TF dose–response curves were observed with increasing amounts of GK-W99R/W167F/W257F, as indicated by indistinguishable Hill coefficients of 1.74 and 1.86 in the presence of GKRP-WT and GKRP-P446L respectively (Figures 5A and 5B, and Table 1). Saturating levels of F6P had no significant effect on the binding of GKRP-WT, but increased the affinity of GKRP-P446L for GK and lowered the degree of co-operativity of the PPI ($H = 1.31$ compared with 1.86). This conclusion was supported by curve fits using simple saturation or sigmoidal functions (Figure 5 and Supplementary Table S6 at http://www.biochemj.org/bj/459/bj4590551add.htm). However, on average, the $S_{0.5}$ value of GK for complex formation of approximately 1.2 μM in the presence of GKRP-WT was 35 % lower than that obtained with GKRP-P446L (Figure 5). Saturating concentrations of glucose, F1P or GKA, either alone or in combination, markedly increased the sigmoidicity of these dose–response curves (Figures 6–8 and Table 1), indicating enhanced co-operativity. In the case of GKRP-WT the effect was most pronounced in the presence of high glucose and GKA, resulting in a 4-fold increase in the $S_{0.5}$ value for GK and a 1.84-fold increase in the Hill coefficient (Figure 6C and Table 1). GKRP-P446L was less responsive to the combined action of saturating glucose and GKA, since the GK $S_{0.5}$ value increased by only 1.73-fold and the Hill coefficient by 1.44-fold (Figure 6D and Table 1). Furthermore, the maximal ΔTF value of GKRP-P446L was generally constant at approximately 0.41–0.44 under all conditions tested, compared with a wider range of 0.29–0.42 for GKRP-WT, depending on the assay conditions. When titration of GKRP-WT with GK was performed in the presence of glucose, F1P or GKA, the TF dose–response curves were shifted to the right and corresponded to changes in the biophysical constants of these ligands largely consistent with known effects (Figures 6–8 and Table 1). The strikingly high efficacy of GKA alone (known not to activate unmodified GK in the absence of glucose [3]) is readily explained by the W99R substitution in GK, the effect of which would be to facilitate access of the GKA to its binding site ([50,51] and Supplementary Online Data). These qualitative and quantitative differences between GKRP-WT and GKRP-P446L are strikingly displayed in Figure 6. The co-operative nature of the GK–GKRP interaction and the extent to which this interaction is modified by physiological ligands and GKAs is further illustrated in Hill plots (Supplementary Figure S9 at http://www.biochemj.org/bj/459/bj4590551add.htm). Since the TF spectra of proteins are influenced by their basic structure and conformational rearrangements upon ligand binding, these results strongly suggest that the P446L substitution on GKRP results in an overall change in structure. We propose that the association of GKRP-P446L with multiple metabolic traits, including reduced T2D risk, can be attributed to its altered overall structure, which acts to hinder GK binding and nuclear import. This hypothesis is supported by the close approximation of Pro^{446} to Asp^{413} (as proposed by Choi et al. [47]) or Gln^{443} (as proposed by Beck et al. [49]), which appear to form a critical salt bridge with Arg^{186} of GK (Figures 1C and 1D).

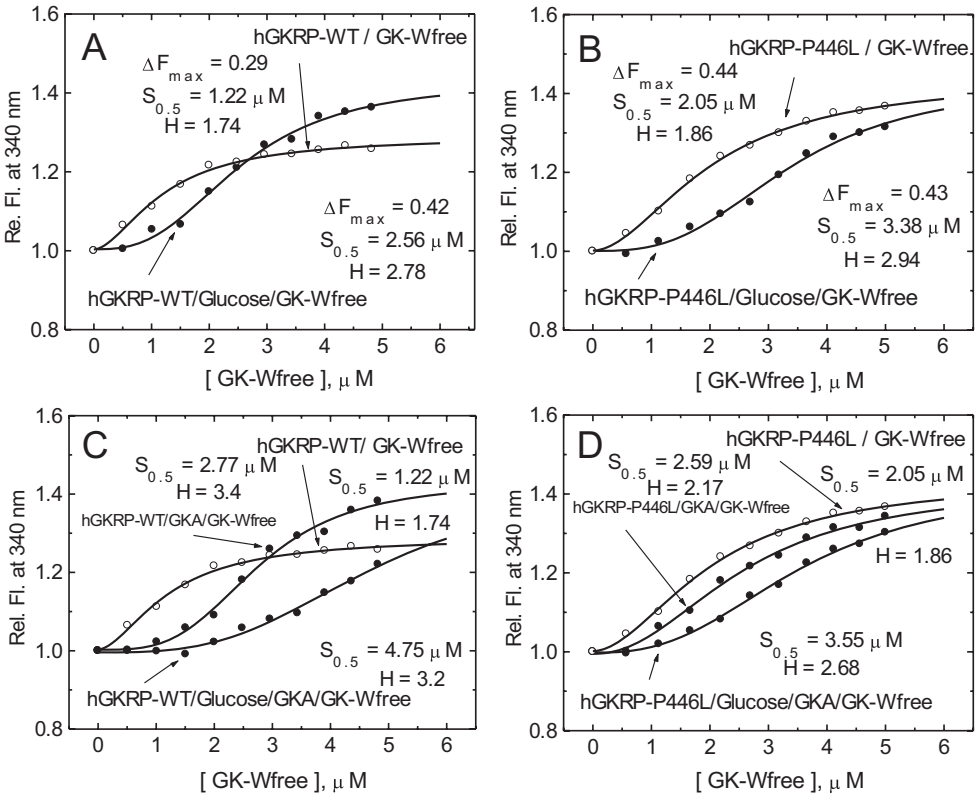

Figure 6 Co-operativity of GK–GKRP complex assembly

(**A** and **B**) Relative TF change for 0.3 μM GKRP in the presence of increasing amounts of GK-W99R/W167F/W257F (GK-Wfree), and in the absence (○) or presence (●) of 100 mM D-glucose for GKRP-WT (**A**) and for GKRP-P446L (**B**). (**C** and **D**) The effect of increasing amounts of GK-W99R/W167F/W257F on the change in TF for 0.5 μM GKRP can be seen in the absence (○) or presence (●) of 20 μM GKA or 20 μM GKA and 100 mM D-glucose for GKRP-WT (**C**) and GKRP-P446L (**D**) ($\lambda_{exc} = 295$ nm; $\lambda_{em} = 340$ nm).

Disassembly of the GK–GKRP complex by glucose, F1P and GKA

Disassembly of the GK–GKRP complex was studied by TF using F1P, glucose and GKA with a GK/GKRP ratio of 3:1, as this ratio most closely mimics the ratio of these two proteins in the cytosol and provided optimal conditions to observe TF changes (see Figure 6). The concentration-dependency curves for these agents were hyperbolic for both GKRP-WT and GKRP-P446L (Tables 2–4 and Supplementary Figures S10–S12 at http://www.biochemj.org/bj/459/bj4590551add.htm). The glucose-dependency curve was monophasic for GKRP-WT, but biphasic for P446L-GKRP (Supplementary Figure S10). An apparent K_d value of 12 mM is consistent with the lower glucose K_d value of 5 mM for unbound GK-W99R/W167F/W257F under these conditions, and reflects the fact that GK-mediated glucose uptake and disposal by the intact hepatocyte is less efficient than expected based on the observed $S_{0.5}$ value for purified GK [9]. The observation of two distinct glucose K_d values in the presence of GKRP-P446L (13.6 and 99.5 mM) is striking. This result is perhaps due to the altered ability of GKRP-P446L to bind glucose besides fructose phosphates (Supplementary Figure S7), which would result in increased, but separate, binding constants for the complex (one for GK and the other for GKRP). GKA was also highly effective in dissociating the GK–GKRP complex, with practically equal K_d values for GKRP-WT and GKRP-P446L (1.49 compared with 1.23 μM) (Supplementary Figure S11 and Table 4). F1P disrupted the 3:1 GK–GKRP complex very effectively (Supplementary Figure S12). However, the apparent K_d values for GKRP-WT and GKRP-P446L differed markedly (127 compared with 298 μM), resembling the 1:2 ratio of the ligand's binding constant for unbound GKRP (65 compared with 139 μM) (Figure 7). The lower affinity of F1P for GK-bound GKRP is likely the result of an altered phosphate ester binding site on GKRP when complexed with GK. We did not study the effect of F6P on complex assembly because the ΔTF value was too small (Figures 7C and 7D).

Table 2 D-Glucose binding by hGKRP (0.3 μM) –GK-W99R/W167F/W257F (1 μM) complexes at 20 °C measured by TF of hGKRP

ΔF is the relative fluorescence change at 340 nm.

Agents	ΔF	K_d (mM)	H	χ^2
GKRP-WT and GK-W99R/W167F/W257F	− 0.065	12	1	2.0×10^{-5}
GKRP-P446L and GK-W99R/W167F/W257F	− 0.064	13.6	1	1.0×10^{-5}
GKRP-P446L and GK-W99R/W167F/W257F	− 0.055	99.5	1	1.3×10^{-5}

Table 3 F1P binding by hGKRP (0.3 μM) –GK-W99R/W167F/W257F (1 μM) at 20 °C measured by TF of hGKRP

ΔF is the relative fluorescence change at 340 nm.

Agents	ΔF	K_d (μM)	H	χ^2
GKRP-WT and GK-W99R/W167F/W257F	− 0.086	127	1	1.0×10^{-5}
GKRP-P446L and GK-W99R/W167F/W257F	− 0.095	298	1	1.0×10^{-5}

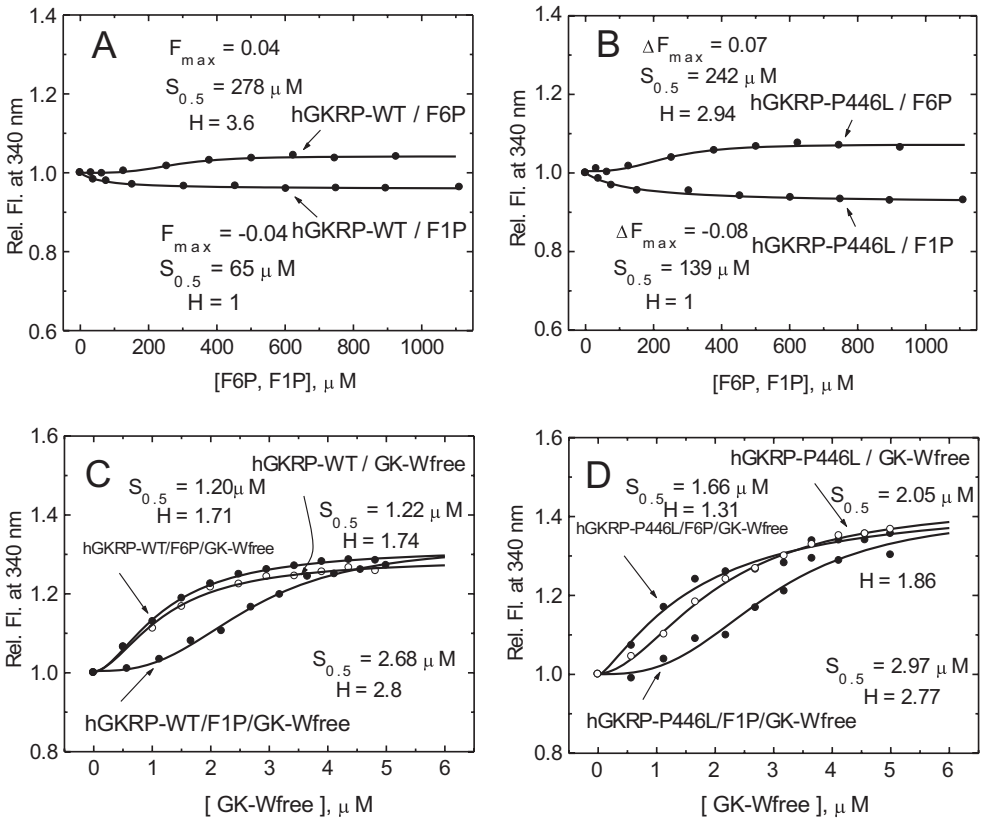

Figure 7 Fructose phosphate ester binding to GKRP and co-operativity of GK–GKRP complex assembly

(**A** and **B**) Relative change in TF for 0.3 μM GKRP in the presence of increasing amounts of F6P and F1P for GKRP-WT (**A**) and GKRP-P446L (**B**). (**C** and **D**) The effect of increasing amounts of GK-W99R/W167F/W257F (GK-Wfree) on the change in TF for 0.5 μM GKRP-WT in the absence (○) or presence (●) of 500 μM F6P or 500 μM F1P for GKRP-WT (**C**) and for GKRP-P446L (**D**) ($\lambda_{exc} = 295$ nm; $\lambda_{em} = 340$ nm).

General discussion and outlook

The potential of TF for studying PPIs

The suitability of TF for structural and functional studies of PPIs depends on the number, location and functional involvement of native tryptophan residues [54]. The present study is the first to apply TF-based methodologies to investigate the GK–GKRP interaction. GK, when investigated in its monomeric form, is highly suitable for such studies due to the large nearly 2-fold increase in TF upon saturation with glucose, as well as the fact that mutation of all three of its native tryptophan residues can be performed without a loss of essential protein function [3,19,21,37,39,43,45,50,51,59,60]. TF studies with GKRP are more challenging because it has six tryptophan residues (Figure 1), one at the N-terminus that is associated with the Lid domain (Trp^{19}), four in its SIS domains (Trp^{222}, Trp^{335}, Trp^{461} and Trp^{484}), and one in the Lid itself (Trp^{517}). The average quantum yield of GKRP is high, allowing for reliable studies at submicromolar protein concentrations, and the fluorescence signals are sufficient to allow for reliable functional and structural analyses. The ability to work with subnanomolar amounts compares favourably with alternative techniques such as crystallography, NMR or isothermal titration calorimetry, which require far more material. In the present study, we show that TF is capable of detecting even subtle conformational changes of GKRP in response to fructose-phosphate esters in agreement with the latest crystallography results [49]. The efficacy of this experimental approach is further demonstrated by its ability to detect qualitative and quantitative TF spectral differences between WT and mutant GKRPs, and to allow analysis of protein unfolding/refolding in the presence of urea. Most significant, this TF-based approach allowed a detailed description of the co-operative nature of GK–GKRP interactions. On the basis of the results already obtained with GK [21,43,50,51] it is anticipated that substitution of single tryptophan residues within GKRP will provide even greater insight into GKRP structure and function. However, the results obtained with GK-W99R/W167F/W257F must be viewed as model studies and their interpretation must be judged carefully because there are some differences compared with WT-GK, i.e. the k_{cat} value and Hill coefficient are reduced and the action of GKA, although highly effective in increasing glucose affinity, has been rendered glucose-independent ([51] and Supplementary Online Data).

The biological relevance of TF in the study of GK–GKRP interactions is also demonstrated upon comparison of our results with previously published data. Anderka et al. [19] characterized complex formation between hepatic GK and GKRP using isothermal titration calorimetry and SPR, and reported dissociation constants of 1–7 μM that are highly comparable with those found in the present study. Choi et al. [47], who used WT recombinant human GK and GKRP, reported K_d values for GK–GKRP complex formation via isothermal titration calorimetry that are consistent with those obtained in the present study. A relatively small contact area of about 2000 Å^2 between the two

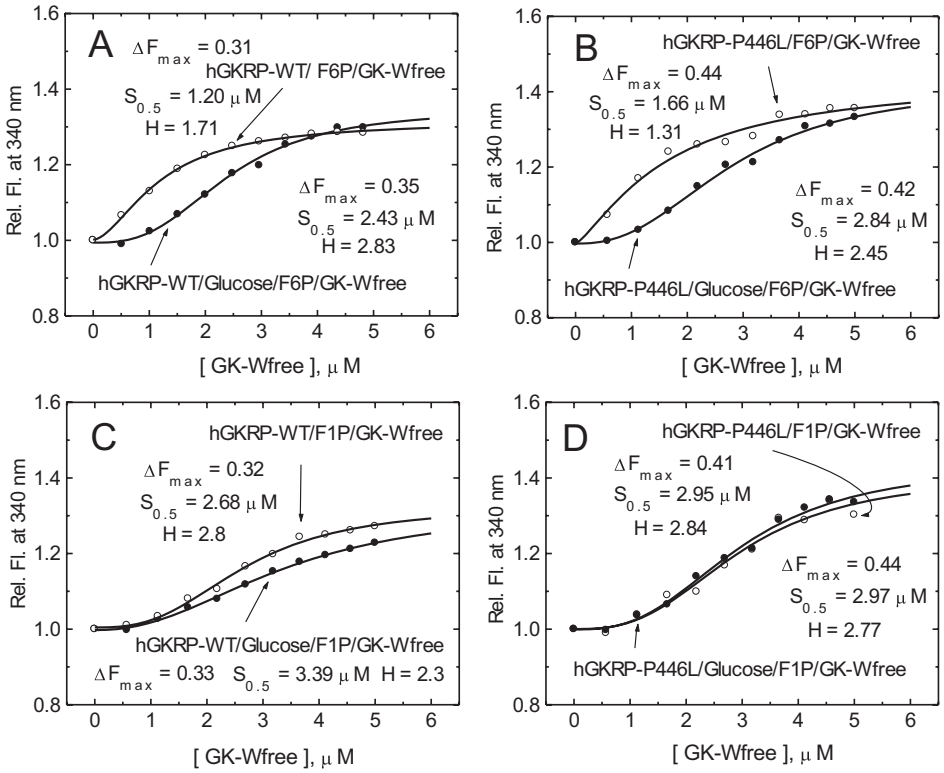

Figure 8 Co-operativity of GK–GKRP complex assembly

(**A** and **B**) Relative change in TF for 0.3 μM GKRP in the presence of increasing amounts of GK-W99R/W167F/W257F (GK-Wfree) on the addition of 500 μM F6P (○) or 500 μM F6P and 100 mM D-glucose (●) for GKRP-WT (**A**) and GKRP-P446L (**B**). (**C** and **D**) The effect of increasing amounts of GK-W99R/W167F/W257F on the change in TF for 0.3 μM GKRP in the presence of 500 μM F1P (○) and 500 μM F1P and 100 mM D-glucose (●) can be seen for GKRP-WT (**C**) and GKRP-P446L (**D**) (λ_{exc} = 295 nm; λ_{em} = 340 nm).

proteins may be the structural prerequisite for a metabolic switch with relatively high association/dissociation rates [19,47,49].

On the biophysical basis of co-operative GK–GKRP interactions and their physiological significance

The observation that GK titration of GKRP results in sigmoidal concentration-dependency curves of increased TF, as well as the fact that this response is exquisitely sensitive to known physiological and pharmacological modifiers of complex assembly and disassembly, suggests a unique biochemical switch mechanism with important physiological implications (Figures 5–8 and Supplementary Figure S9). The shift in the GK dose–response curve to the right, combined with a large increase in the Hill coefficient in response to glucose, F1P and GKA, either alone or in combination, demonstrates that modulator molecules are particularly effective when cytosolic GK levels are low, i.e. when GK is retained in an inactive nuclear complex with GKRP. Modulation of this switch would result in corresponding equilibrium shifts between cytosolic and nuclear pools of GK. The K_d values of the small molecule modulators shown in the present paper are consistent with this interpretation (Tables 2–4 and Supplementary Figures S10–S12). We can only speculate about the biophysical basis of formation of this co-operative complex. The explanation may lie in the hysteretic behaviour of GK, as suggested by Bourbonais et al. [61], that GK release from GKRP in response to glucose is a slow process, exemplified by reaction progress curves with transition kinetics resembling those of activated or deactivated GK in response to glucose [3,17,41,45, 51,61] (Supplementary Figure S13 at http://www.biochemj.org/bj/459/bj4590551add.htm).

Table 4 GKA binding by hGKRP (0.3 μM)–GK-W99R/W167F/W257F (1 μM) complexes at 20 °C measured by TF of hGKRP

ΔF is the relative fluorescence change at 340 nm.

Agents	ΔF	K_d (μM)	H	χ^2
GKRP-WT and GK-W99R/W167F/W257F	− 0.084	1.49	1	3.2×10^{-5}
GKRP-P446L and GK-W99R/W167F/W257F	− 0.065	1.23	1	1.0×10^{-5}

The molecular basis of GK trafficking in hepatocytes during fasting and refeeding

The acute regulation of hepatic GK in response to feeding and fasting is poorly understood, partly due to the added complexity of altered subcellular compartmentalization of GK in response to these conditions and also because of the impact that the glucose-6-phosphatase system of the endoplasmic reticulum may have on glucose and glucose 6-phosphate levels and glucose uptake and release [7,62]. On the basis of the evidence that the cytosolic GKRP concentration appears to be much lower than that in the nucleus, but still appears to be essential for the interaction between GK and the NPC [1,2,10,11], we studied GK–GKRP interactions as they might occur in the cytosol at ratios ranging from 1:1 to 10:1 [1,2,9]. This approach demonstrated a sigmoidal GK

dependency of complex formation, with Hill coefficients ranging from 1.3 to 3.2 depending on the experimental conditions. This suggests that GK binding to and release from GKRP functions as a co-operative switch that is activated by high levels of glucose, F1P, and pharmacological agents such as GKAs and GKRPIs, and is deactivated by low levels of these compounds. This critical step in glucose homoeostasis is thus analogous to that observed in the classical oxygen loading and releasing function of haemoglobin [63]. A similar co-operative switch in GK–GKRP assembly and disassembly can be postulated to exist in the nuclear space, which is readily accessible to low-molecular-mass ligands and consequently provides the molecular explanation for the compartmental reshuffling of GK during feeding–fasting transitions [1,2,8–11]. This subcellular redistribution of GK implies the rapid movement of significant amounts of protein and considerable expenditure of metabolic energy. A dramatic change in the equilibrium of the GK–GKRP complex must occur to allow for the timely and efficient subcellular redistribution of GK in this manner.

Pathophysiological and pharmacological significance of the hepatic GK–GKRP switch

Activation of the GK–GKRP switch by F1P is not only of physiological significance, but could also be instrumental in the metabolic dysregulation that results from excessive dietary fructose intake, which is hypothesized to be a major contributor to metabolic diseases such as obesity and T2D [64–66]. Fructose levels of 1 mM or more in the portal vein would result in a high degree of F1P production by hepatic fructokinase C, greatly enhancing GK mobilization and activation. This hyperactivation of GK would result in increased glycolysis, glycogen synthesis and *de novo* lipogenesis, all of which may contribute to increased insulin resistance, obesity, hepatosteatosis and T2D [67]. Excessive activation of the GK–GKRP switch by F1P may also amplify other cellular mechanisms (such as ATP depletion and uric acid overproduction) that could contribute to disease progression [65]. In contrast, low amounts of fructose appear to have a beneficial effect on hepatic glucose metabolism [68,69], rendering the GK–GKRP switch optimal in its ability to respond to common carbohydrate meals that contain both sucrose and starches. In the context of GKAs, a recent report of a Phase II trial of subjects with T2D treated with the GKA MK0941 observed that a low dose of the drug resulted in a slow-onset long-lasting beneficial effect, whereas higher doses of the drug resulted in fast-onset transient effects associated with an increase in blood lipids and cardiovascular side effects [34]. Extrapolating from these clinical results with a GKA indicates that similar difficulties might be encountered with the newly discovered GKRPIs when applied to treat human disease [22].

Contribution to our understanding of the molecular mechanisms explaining genetic associations of the GKRP-P449L variant with metabolic traits and diabetes risk

Kinetic studies of GKRP-P446L have demonstrated a reduced ability of this variant protein to inhibit GK as a consequence of reduced responsiveness to F6P, and cellular studies have shown impaired GK binding and nuclear storage [28,30,31]. Subsequent alterations in GK localization and activity may explain the association of this GKRP variant with metabolic traits such as fasting glucose and triacylglycerol levels [33]. The present study expands the characterization of GKRP-P446L. First, we show that structural instability or impaired protein folding are unlikely to be major contributors to GKRP-P446L dysfunction (Figure 4). Secondly, the increase in the GK $S_{0.5}$ value for binding to GKRP-P446L, the reduced affinity of GK for GKRP-P446L in the presence of high glucose and GKA, the abnormal constancy of TF maxima under various conditions, and, finally, the reduced co-operativity with GK, suggest a narrower conformational range for this variant protein (Figures 5–8 and Table 1, and Supplementary Figure S9). There is also evidence for reduced fructose-phosphate ester binding by GKRP-P446L (Supplementary Figure S12). Taken together, these data indicate significant conformational differences as a result of the P446L substitution, which could limit the ability of GKRP to facilitate nuclear uptake of GK via the NPC and act as an effective storage partner in the nucleus. The recently disclosed crystal structure of human GKRP and the binary xGK–xGKRP and hGK–rGKRP complex [47–49] suggests that Pro^{446} is located in one of the surface loops of the SIS-2 domain, a region with high surface entropy, that may explain both the conformational and functional alterations observed in the present study (Figures 1 and 9). Proline is a helix-disrupting amino acid [70], and replacing it with leucine may destabilize this region.

In Figure 9, the results of our previous mutational analyses of the GK–GKRP interaction [21] are integrated with recent crystallographic information [47–49]. This clearly shows that the SIS-2 region is involved directly in GKRP binding to GK [47,49]. The GKRP-binding site is located between two groups of amino acids, composed of Glu^{51} and Glu^{52} in the large lobe and Lys^{140}–Leu^{144} and Met^{197} in the small lobe. Both patches are clearly separate to the GKA-binding site (Figure 9A). Activation of GK by glucose or GKAs results in a large spatial separation of these two groups which would dislodge GKRP (Figure 9B). Figures 9(C) and 9(D) further illustrate how the large conformational change in GK in response to glucose is the main driving force behind disruption of the inactive GK–GKRP complex. The position of Pro^{446} on the surface of GKRP and its close vicinity to Asp^{413} [47] and Gln^{443} [49], which appear to form a salt bridge with Arg^{186} of GK, is almost certainly of functional significance, and the P446L substitution may thus interfere directly with binding to GK (compare with Figure 1D). The widely dispersed intramolecular locations of 16 other rare GKRP variants associated with serum triacylglycerol levels, and their spatial relationship to the allosteric fructose phosphate-, GKRPI- and GK-binding sites, suggests that the molecular mechanisms that underpin these mutants differ greatly (Figure 1C). Further pursuit of TF in the study of rare genetic variants in GKRP promises to be useful in understanding these distinct molecular mechanisms in greater depth.

Outlook

The results of the present study suggest that TF is an excellent means to improve our understanding of GKRP structure and function and its interaction with GK. Exploration of the co-operative nature of the GK–GKRP interaction using rapid mixing studies may better resolve the apparent slow transition of GKRP binding to and dissociation from GK. Such studies may also be extended to other disease-associated GKRP variants found in humans. Also, utilization of our advanced biophysical knowledge of the GK–GKRP interaction as a co-operative metabolite- and drug-responsive switch will deepen our understanding of the physiological chemistry and pharmacology of hepatic glucose metabolism and its contribution to disease pathology.

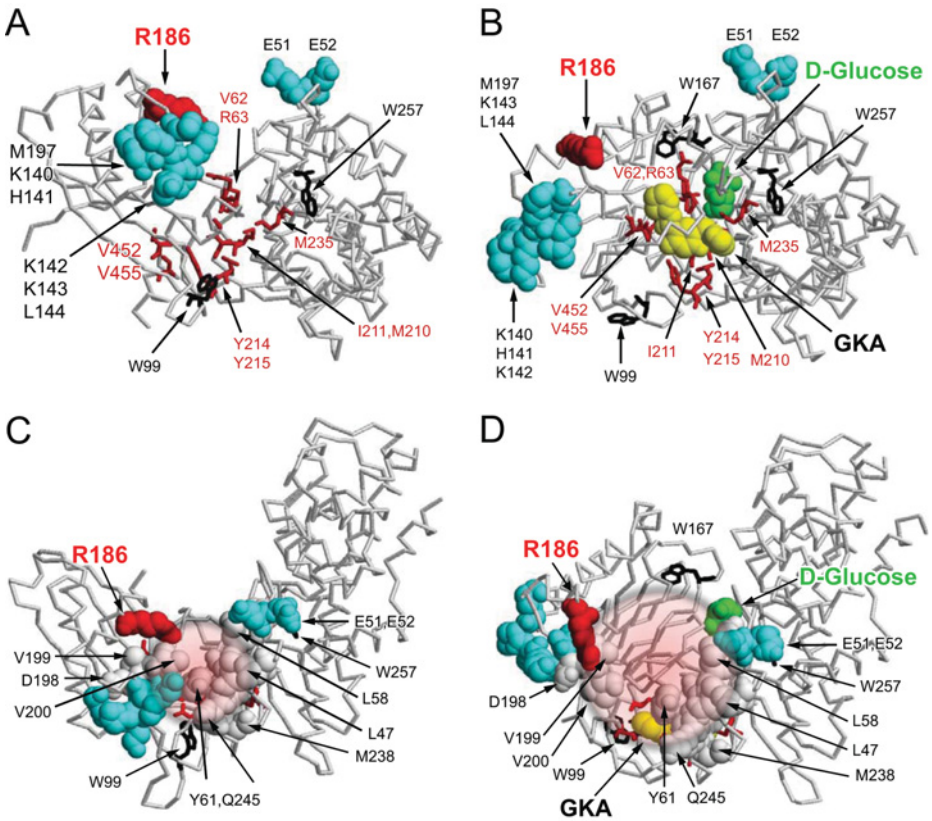

Figure 9 Effects of glucose, fructose-phosphate esters, GKAs and GKRPIs on the GK–GKRP complex

The Figure summarizes the structural information on the GK–GKRP complex under the influence of glucose and known allosteric ligands of the two participating proteins ([21,22,38,47–49] and the present study). (**A** and **B**) The results of mutational analyses [21]. (**C** and **D**) The combined results of mutational [21] and crystallographic [22,47–49] analyses of these interactions [note that the orientation differs from that of (**A**) and (**B**) (an approximately 90° rotation towards the face of the page) in order to emphasize that the site of GK–GKRP interaction is distinct from that of GK–GKA]. All structural information is projected on to the GK structures published by Kamata et al. [38], and the tryptophan residues are depicted as black stick structures for improved orientation. (**A**) The allosteric modifier region of GK with two distinct binding sites for GKRP and GKA in the open conformation. Amino acids that affect interaction with GKRP are shown as space-filled structures in cyan. Arg^{186} of GK is presented in magenta [47,49] to show its close vicinity to other amino acids in the small lobe of GK that have been implicated in GKRP binding. GKA-contacting amino acids are shown as red stick models. Activation of GK by glucose (green) combined with a GKA (yellow) profoundly alters the proposed GKRP-binding site by affecting groups of amino acids involved in binding including the critical Trp^{99} for binding (**B**). (**C** and **D**) The allosteric binding site for GKRP is indicated in grey space-filled structures for eight of the 15 identified contact amino acids [47,49]. Amino acids immediately surrounding the GKRP contact site are those identified by mutational analysis to influence GKRP binding to GK and are presented as space-filled structures in cyan (see also **A** and **B**) [21]. The GK-binding site for GKRP is drawn schematically as a small circular patch in (**C**) to delineate where the two proteins interact in the complex and a larger patch in (**D**) to delineate the conformational change that dislodges the inhibitor when glucose and/or GKA are bound to GK.

AUTHOR CONTRIBUTION

Anne Raimondo and Amy Barrett generated the human recombinant GKRP proteins. Anna Gloyn contributed to the study design and data interpretation. Anne Raimondo and Anna Gloyn contributed to writing the paper. Bogumil Zelent performed the TF studies, generated the numerical and graphic presentation of the results, and contributed to writing the paper. Carol Buettger and Pan Chen generated the human GK proteins. Franz Matschinsky conceptualized and supervised the study, generated the first draft and helped finalize the paper. All authors approved the final version of the paper.

FUNDING

This work was supported by the NIDDK (National Institute of Diabetes and Digestive and Kidney Diseases) [grant number 22122 (to F.M.M.)], Elke Matschinsky and the Wellcome Trust [grant number 095101/Z/10/Z]. A.L.G. is a Wellcome Trust Senior Fellow in Basic and Biomedical Science.

REFERENCES

1 Agius, L. (2008) Glucokinase and molecular aspects of liver glycogen metabolism. Biochem. J. **414**, 1–18
2 Iynedjian, P. B. (2009) Molecular physiology of mammalian glucokinase. Cell. Mol. Life Sci. **66**, 27–42
3 Matschinsky, F. M., Zelent, B., Doliba, N. M., Kaestner, K. H., Vanderkooi, J. M., Grimsby, J., Berthel, S. J. and Sarabu, R. (2011) Research and development of glucokinase activators for diabetes therapy: theoretical and practical aspects. Handb. Exp. Pharmacol. **203**, 357–401
4 Wilson, J. E. (1995) Hexokinases. Rev. Physiol. Biochem. Pharmacol. **126**, 65–198
5 Cornish-Bowden, A. and Cardenas, M. L. (2004) Glucokinase: a monomeric enzyme with postitive co-operativity. In Glucokinase and Glycaemic Diseases: From Basics to Novel Therapuetics (Matschinsky, F. and Magnuson, M. A., eds), pp. 125–134, Karger, Basel
6 Postic, C., Decaux, J. F. and Girard, J. (2004) Regulation of hepatic glucokinase gene expression. In Glucokinase and Glycaemic Disease: From Basic to Therapeutics (Matschinsky, F. M. and Magnuson, M. A., eds), pp. 180–192, Karger, Basel
7 Postic, C., Dentin, R. and Girard, J. (2004) Role of the liver in the control of carbohydrate and lipid homeostasis. Diabet. Metab. **30**, 398–408
8 Toyoda, Y., Miwa, I., Satake, S., Anai, M. and Oka, Y. (1995) Nuclear location of the regulatory protein of glucokinase in rat liver and translocation of the regulator to the cytoplasm in response to high glucose. Biochem. Biophys. Res. Commun. **215**, 467–473
9 Van Schaftingen, E. and Vega-da-Cunha, M. (2004) Discovery and role of glucokinase regulatory protein. In Glucokinase and Glycaemic Disease From Basic to Therapeutics (Matschinsky, F. M. and Magnuson, M. A., eds), pp. 193–107, Karger, Basel
10 Bosco, D., Meda, P. and Iynedjian, P. B. (2000) Glucokinase and glucokinase regulatory protein: mutual dependence for nuclear localization. Biochem. J. **348**, 215–222

11 Shiota, C., Coffey, J., Grimsby, J., Grippo, J. F. and Magnuson, M. A. (1999) Nuclear import of hepatic glucokinase depends upon glucokinase regulatory protein, whereas export is due to a nuclear export signal sequence in glucokinase. J. Biol. Chem. **274**, 37125–37130

12 Brocklehurst, K. J., Davies, R. A. and Agius, L. (2004) Differences in regulatory properties between human and rat glucokinase regulatory protein. Biochem. J. **378**, 693–697

13 Vandercammen, A. and Van Schaftingen, E. (1993) Species and tissue distribution of the regulatory protein of glucokinase. Biochem. J. **294**, 551–556

14 Filipski, K. J., Stevens, B. D. and Pfefferkorn, J. F. (2012) Glucokinase activators in development. In New Strategies for Type 2 Diabetes (Small Molecule Approach) (Jones, R. M., ed.), pp. 88–100, RSC Publishing, London

15 Grimsby, J., Sarabu, R., Corbett, W. L., Haynes, N. E., Bizzarro, F. T., Coffey, J. W., Guertin, K. R., Hilliard, D. W., Kester, R. F., Mahaney, P. E. et al. (2003) Allosteric activators of glucokinase: potential role in diabetes therapy. Science **301**, 370–373

16 Matschinsky, F. M. (2009) Assessing the potential of glucokinase activators in diabetes therapy. Nat. Rev. Drug Discov. **8**, 399–416

17 Matschinsky, F. M., Zelent, B., Doliba, N., Li, C., Vanderkooi, J. M., Naji, A., Sarabu, R. and Grimsby, J. (2011) Glucokinase activators for diabetes therapy: May 2010 status report. Diabet. Care **34**, S236–S243

18 Matschinsky, F. M. (2013) GKAs for diabetes therapy: why no clinically useful drug after two decades of trying? Trends Pharmacol. Sci. **34**, 90–99

19 Anderka, O., Boyken, J., Aschenbach, U., Batzer, A., Boscheinen, O. and Schmoll, D. (2008) Biophysical characterization of the interaction between hepatic glucokinase and its regulatory protein: impact of physiological and pharmacological effectors. J. Biol. Chem. **283**, 31333–31340

20 Futamura, M., Hosaka, H., Kadotani, A., Shimazaki, H., Sasaki, K., Ohyama, S., Nishimura, T., Eiki, J. and Nagata, Y. (2006) An allosteric activator of glucokinase impairs the interaction of glucokinase and glucokinase regulatory protein and regulates glucose metabolism. J. Biol. Chem. **281**, 37668–37674

21 Zelent, B., Odili, S., Buettger, C., Zelent, D. K., Chen, P., Fenner, D., Bass, J., Stanley, C., Laberge, M., Vanderkooi, J. M. et al. (2011) Mutational analysis of allosteric activation and inhibition of glucokinase. Biochem. J. **440**, 203–215

22 Lloyd, D. J., St Jean, Jr, D. J., Kurzeja, R. J. M., Wahl, R. C., Michelsen, K., Cupples, R., Chen, M., Wu, J., Sivits, G., Helmering, J. et al. (2013) Antidiabetic effects of glucokinase regulatory protein small-molecule disruptors. Nature **504**, 437–440

23 Baic, D., Ladewski, B. G. and Frye, B. E. (1979) Quantitative ultrastructural studies of hepatocytes from fed and starved frogs. J. Exp. Zool. **210**, 381–406

24 Riede, U. N., Hodel, J., Matt, C. V., Rasser, Y. and Rohr, H. P. (1973) Influence of starvation on the quantitative cytoarchitectur of the rat liver cell. II. Chronic partial starvation. Beitrage zur Pathologie **150**, 246–260

25 Froguel, P., Vaxillaire, M., Sun, F., Velho, G., Zouali, H., Butel, M. O., Lesage, S., Vionnet, N., Clement, K., Fougerousse, F. et al. (1992) Close linkage of glucokinase locus on chromosome 7p to early-onset non-insulin-dependent diabetes mellitus. Nature **356**, 162–164

26 Glaser, B., Kesavan, P., Heyman, M., Davis, E., Cuesta, A., Buchs, A., Stanley, C. A., Thornton, P. S., Permutt, M. A., Matschinsky, F. M. and Herold, K. C. (1998) Familial hyperinsulinism caused by an activating glucokinase mutation. N. Engl. J. Med. **338**, 226–230

27 Njolstad, P. R., Sovik, O., Cuesta-Munoz, A., Bjorkhaug, L., Massa, O., Barbetti, F., Undlien, D. E., Shiota, C., Magnuson, M. A., Molven, A. et al. (2001) Neonatal diabetes mellitus due to complete glucokinase deficiency. N. Engl. J. Med. **344**, 1588–1592

28 Beer, N. L., Tribble, N. D., McCulloch, L. J., Roos, C., Johnson, P. R., Orho-Melander, M. and Gloyn, A. L. (2009) The P446L variant in GCKR associated with fasting plasma glucose and triglyceride levels exerts its effect through increased glucokinase activity in liver. Hum. Mol. Genet. **18**, 4081–4088

29 Osbak, K. K., Colclough, K., Saint-Martin, C., Beer, N. L., Bellanne-Chantelot, C., Ellard, S. and Gloyn, A. L. (2009) Update on mutations in glucokinase (GCK), which cause maturity-onset diabetes of the young, permanent neonatal diabetes, and hyperinsulinemic hypoglycemia. Hum. Mut. **30**, 1512–1526

30 Rees, M. G., Ng, D., Ruppert, S., Turner, C., Beer, N. L., Swift, A. J., Morken, M. A., Below, J. E., Blech, I., Mullikin, J. C. et al. (2012) Correlation of rare coding variants in the gene encoding human glucokinase regulatory protein with phenotypic, cellular, and kinetic outcomes. J. Clin. Invest. **122**, 205–217

31 Rees, M. G., Wincovitch, S., Schultz, J., Waterstradt, R., Beer, N. L., Baltrusch, S., Collins, F. S. and Gloyn, A. L. (2012) Cellular characterisation of the GCKR P446L variant associated with type 2 diabetes risk. Diabetologia **55**, 114–122

32 Johansen, C. T., Wang, J., Lanktree, M. B., Cao, H., McIntyre, A. D., Ban, M. R., Martins, R. A., Kennedy, B. A., Hassell, R. G., Visser, M. E. et al. (2010) Excess of rare variants in genes identified by genome-wide association study of hypertriglyceridemia. Nat. Genet. **42**, 684–687

33 Orho-Melander, M., Melander, O., Guiducci, C., Perez-Martinez, P., Corella, D., Roos, C., Tewhey, R., Rieder, M. J., Hall, J., Abecasis, G. et al. (2008) Common missense variant in the glucokinase regulatory protein gene is associated with increased plasma triglyceride and C-reactive protein but lower fasting glucose concentrations. Diabetes **57**, 3112–3121

34 Meininger, G. E., Scott, R., Alba, M., Shentu, Y., Luo, E., Amin, H., Davies, M. J., Kaufman, K. D. and Goldstein, B. J. (2011) Effects of MK-0941, a novel glucokinase activator, on glycemic control in insulin-treated patients with type 2 diabetes. Diabet. Care **34**, 2560–2566

35 Antoine, M., Boutin, J. A. and Ferry, G. (2009) Binding kinetics of glucose and allosteric activators to human glucokinase reveal multiple conformational states. Biochemistry **48**, 5466–5482

36 Frieden, C. (1979) Slow transitions and hysteretic behavior in enzymes. Ann. Rev. Biochem. **48**, 471–489

37 Heredia, V. V., Carlson, T. J., Garcia, E. and Sun, S. (2006) Biochemical basis of glucokinase activation and the regulation by glucokinase regulatory protein in naturally occurring mutations. J. Biol. Chem. **281**, 40201–40207

38 Kamata, K., Mitsuya, M., Nishimura, T., Eiki, J. and Nagata, Y. (2004) Structural basis for allosteric regulation of the monomeric allosteric enzyme human glucokinase. Structure **12**, 429–438

39 Larion, M. and Miller, B. G. (2010) Global fit analysis of glucose binding curves reveals a minimal model for kinetic cooperativity in human glucokinase. Biochemistry **49**, 8902–8911

40 Larion, M., Salinas, R. K., Bruschweiler-Li, L., Bruschweiler, R. and Miller, B. G. (2010) Direct evidence of conformational heterogeneity in human pancreatic glucokinase from high-resolution nuclear magnetic resonance. Biochemistry **49**, 7969–7971

41 Lin, S. X. and Neet, K. E. (1990) Demonstration of a slow conformational change in liver glucokinase by fluorescence spectroscopy. J. Biol. Chem. **265**, 9670–9675

42 Liu, S., Ammirati, M. J., Song, X., Knafels, J. D., Zhang, J., Greasley, S. E., Pfefferkorn, J. A. and Qiu, X. (2012) Insights into mechanism of glucokinase activation: observation of multiple distinct protein conformations. J. Biol. Chem. **287**, 13598–13610

43 Molnes, J., Bjorkhaug, L., Sovik, O., Njolstad, P. R. and Flatmark, T. (2008) Catalytic activation of human glucokinase by substrate binding: residue contacts involved in the binding of D-glucose to the super-open form and conformational transitions. FEBS J. **275**, 2467–2481

44 Neet, K. E. and Ainslie, Jr, G. R. (1980) Hysteretic enzymes. Methods Enzymol. **64**, 192–226

45 Neet, K. E., Keenan, R. P. and Tippett, P. S. (1990) Observation of a kinetic slow transition in monomeric glucokinase. Biochemistry **29**, 770–777

46 Cornish-Bowden, A. (1995) Fundamental Enzyme Kinetics, Portland Press, London

47 Choi, J. M., Seo, M. H., Kyeong, H. H., Kim, E. and Kim, H. S. (2013) Molecular basis for the role of glucokinase regulatory protein as the allosteric switch for glucokinase. Proc. Natl. Acad. Sci. U.S.A. **110**, 10171–10176

48 Pautsch, A., Stadler, N., Lohle, A., Rist, W., Berg, A., Glocker, L., Nar, H., Reinert, D., Lenter, M., Heckel, A. et al. (2013) Crystal structure of glucokinase regulatory protein. Biochemistry **52**, 3523–3531

49 Beck, T. and Miller, B. G. (2013) Structural basis for regulation of human glucokinase by glucokinase regulatory protein. Biochemistry **52**, 6232–6239

50 Zelent, B., Buettger, C., Grimsby, J., Sarabu, R., Vanderkooi, J. M., Wand, A. J. and Matschinsky, F. M. (2012) Thermal stability of glucokinase (GK) as influenced by the substrate glucose, an allosteric glucokinase activator drug (GKA) and the osmolytes glycerol and urea. Biochim. Biophy. Acta **1824**, 769–784

51 Zelent, B., Odili, S., Buettger, C., Shiota, C., Grimsby, J., Taub, R., Magnuson, M. A., Vanderkooi, J. M. and Matschinsky, F. M. (2008) Sugar binding to recombinant wild-type and mutant glucokinase monitored by kinetic measurement and tryptophan fluorescence. Biochem. J. **413**, 269–280

52 Liang, Y., Kesavan, P., Wang, L. Q., Niswender, K., Tanizawa, Y., Permutt, M. A., Magnuson, M. A. and Matschinsky, F. M. (1995) Variable effects of maturity-onset-diabetes-of-youth (MODY)-associated glucokinase mutations on substrate interactions and stability of the enzyme. Biochem. J. **309**, 167–173

53 Davis, E. A., Cuesta-Munoz, A., Raoul, M., Buettger, C., Sweet, I., Moates, M., Magnuson, M. A. and Matschinsky, F. M. (1999) Mutants of glucokinase cause hypoglycaemia and hyperglycaemia syndromes and their analysis illuminates fundamental quantitative concepts of glucose homeostasis. Diabetologia **42**, 1175–1186

54 Lakowicz, J. R. (2006) Prinicples of Fluorescence Spectorscopy, 3rd ed., Springer, New York

55 Szabo, A. G. and Rayner, D. M. (1980) Fluorescence decay of tryptophan conformers in aquesous solutions. J. Am. Chem. Soc. **102**, 554–563

56 Mach, H., Middaugh, C. R. and Lewis, R. V. (1992) Statistical determination of the average values of the extinction coefficients of tryptophan and tyrosine in native proteins. Anal. Biochem. **200**, 74–80

57 Zelent, B., Veklich, Y., Murray, J., Parkes, J. H., Gibson, S. and Liebman, P. A. (2001) Rapid irreversible G protein alpha subunit misfolding due to intramolecular kinetic bottleneck that precedes Mg^{2+} "lock" after GTP/GDP exchange. Biochemistry **40**, 9647–9656
58 Steinfeld, J., Francisco, J. S. and Hase, W. L. (1989) Chemical Kinetics and Dynamics, Prentice-Hall, New Jersey
59 Fenner, D., Odili, S., Hong, H. K., Kobayashi, Y., Kohsaka, A., Siepka, S. M., Vitaterna, M. H., Chen, P., Zelent, B., Grimsby, J. et al. (2011) Generation of *N*-ethyl-*N*-nitrosourea (ENU) diabetes models in mice demonstrates genotype-specific action of glucokinase activators. J. Biol. Chem. **286**, 39560–39572
60 Zhang, J., Li, C., Chen, K., Zhu, W., Shen, X. and Jiang, H. (2006) Conformational transition pathway in the allosteric process of human glucokinase. Proc. Natl. Acad. Sci. U.S.A. **103**, 13368–13373
61 Bourbonais, F. J., Chen, J., Huang, C., Zhang, Y., Pfefferkorn, J. A. and Landro, J. A. (2012) Modulation of glucokinase by glucose, small-molecule activator and glucokinase regulatory protein: steady-state kinetic and cell-based analysis. Biochem. J. **441**, 881–887
62 van Schaftingen, E. and Gerin, I. (2002) The glucose-6-phosphatase system. Biochem. J. **362**, 513–532
63 Yonetani, T. and Kanaori, K. (2013) How does hemoglobin generate such diverse functionality of physiological relevance? Biochim. Biophys. Acta **1834**, 1873–1884
64 Bray, G. A. (2013) Energy and fructose from beverages sweetened with sugar or high-fructose corn syrup pose a health risk for some people. Adv. Nutr. **4**, 220–225
65 Johnson, R. J., Perez-Pozo, S. E., Sautin, Y. Y., Manitius, J., Sanchez-Lozada, L. G., Feig, D. I., Shafiu, M., Segal, M., Glassock, R. J., Shimada, M. et al. (2009) Hypothesis: could excessive fructose intake and uric acid cause type 2 diabetes? Endocr. Rev. **30**, 96–116
66 White, J. S. (2013) Challenging the fructose hypothesis: new perspectives on fructose consumption and metabolism. Adv. Nutr. **4**, 246–256
67 Nissim, I., Horyn, O., Daikhin, Y., Wehrli, S. L., Yudkoff, M. and Matschinsky, F. M. (2012) Effects of a glucokinase activator on hepatic intermediary metabolism: study with 13C-isotopomer-based metabolomics. Biochem. J. **444**, 537–551
68 Cozma, A. I., Sievenpiper, J. L., de Souza, R. J., Chiavaroli, L., Ha, V., Wang, D. D., Mirrahimi, A., Yu, M. E., Carleton, A. J., Di Buono, M. et al. (2012) Effect of fructose on glycemic control in diabetes: a systematic review and meta-analysis of controlled feeding trials. Diabet. Care **35**, 1611–1620
69 Shiota, M., Moore, M. C., Galassetti, P., Monohan, M., Neal, D. W., Shulman, G. I. and Cherrington, A. D. (2002) Inclusion of low amounts of fructose with an intraduodenal glucose load markedly reduces postprandial hyperglycemia and hyperinsulinemia in the conscious dog. Diabetes **51**, 469–478
70 Wedemeyer, W. J., Welker, E. and Scheraga, H. A. (2002) Proline *cis–trans* isomerization and protein folding. Biochemistry **41**, 14637–14644

Received 11 October 2013/3 February 2014; accepted 26 February 2014
Published as BJ Immediate Publication 26 February 2014, doi:10.1042/BJ20131363

Biochem. J. (2014) **459**, 551–564 (Printed in Great Britain) doi:10.1042/BJ20131363

online data

SUPPLEMENTARY ONLINE DATA

Analysis of the co-operative interaction between the allosterically regulated proteins GK and GKRP using tryptophan fluorescence

Bogumil ZELENT*, Anne RAIMONDO†, Amy BARRETT†, Carol W. BUETTGER*, Pan CHEN*, Anna L. GLOYN† and Franz M. MATSCHINSKY*[1]

*Department of Biochemistry and Biophysics and Institute for Diabetes, Obesity and Metabolism, Perelman School of Medicine, University of Pennsylvania, Philadelphia, PA, U.S.A.
†Oxford Centre for Diabetes Endocrinology & Metabolism, University of Oxford, Oxford, U.K.

RESULTS AND DISCUSSION

Co-operativity and allostery in GK–GKRP complex formation: conceptual and terminological considerations

The present study describes experiments which demonstrate that the concentration-dependency curve characterizing binding of GK by GKRP is sigmoidal deviating from a classical hyperbolic binding isotherm. TF of GKRP, which contains six tryptophan residues distributed throughout the molecule, was used as a sensitive indicator of this interaction with a non-fluorescent GK reagent (Figure S1A). Glucose, F1P, a drug that activates GK (a GKA) and various combinations of these magnified this sigmoidicity manifold resulting in very steep effector-dependency curves manifesting switch characteristics (Figures S5–S8). This phenomenology is strikingly illustrated by the summary of the results in linearized plots using the Hill equation (Supplementary Figure S9). Such phenomenology is commonly characterized by the concepts of co-operativity and allostery, best exemplified by oxygen binding to haemoglobin. The classical models of Monod–Wyman–Changeux (the MWC selection or symmetry model [1]) and of Koshland–Nemethy–Filmer (the KNF instruction or sequential model [2]) are commonly used to provide mechanistic explanations for co-operativity and allostery. An essential common postulate of these two models is the oligomeric nature of the proteins exhibiting co-operativity. Allostery, the other common feature of these models (a term derived from the Greek and meaning 'of different shape'), refers to the fact that proteins may be regulated by molecules that differ structurally from the substrate of an enzyme or target of a regulatory protein implying also the existence of a separate binding site [3].

The method of choice would be to apply approved concepts of co-operativity and allostery (the MWC and KNF models) for understanding at the molecular level the sigmoidicity of the concentration-dependency curve for assembly of the GK–GKRP complex, but this presents difficulties because of the unique biochemistry and monomeric nature of the two binding partners of the complex. The catalytic function of GK clearly shows co-operativity and allostery. The concentration-dependency curve for glucose binding to GK is, however, hyperbolic as expression of a single binding site of the monomeric enzyme, whereas that for phosphorylation of glucose by GK in the presence of Mg-ATP is sigmoidal/co-operative [4], which is explained kinetically by two related models termed the LIST (ligand-induced slow transition) [5,6] and the mnemonic [7,8] models respectively, both of which are based on the hysteretic nature of the protein [7,8]; hysteresis referring to the fact that the ligand-induced transition from low-affinity to high-affinity conformations of the protein is slow compared with its k_{cat} value [5,7,9]. GK has a well-defined allosteric modifier region remote from the active site with two distinct receptors for GKA and GKRP, one activating the other inhibiting the enzyme [10,11]. An additional allosteric site was recently identified that binds the proapoptotic factor BAD which increases the V_{max} value when occupied [12]. GKRP also clearly shows co-operativity and allostery. The 'active site' of GKRP mediates binding to its receptor on GK. The binding curve is sigmoidal/co-operative as described in the present paper and by Choi et al. [13]. GKRP has two separate allosteric sites, one binding fructose-phosphate esters [13,14] which either enhance (fructose 6-phosphate) or inhibit (fructose 1-phosphate) binding to GK (to result in opposite TF changes of GKRP; Figure S7) and the other binding a pharmacological disruptor of the GK–GKRP complex [15], in the present paper referred to as GKRPIs and discussed in the legend of Figure S1.

The Hill equation, first published 100 years ago as a purely descriptive formula to characterize co-operativity of oxygen binding to haemoglobin [16,17], allows us to describe similarly the co-operative interaction of the GK and GKRP monomers as influenced by glucose (binding to the substrate site of GK) and various allosteric effector molecules (fructose-phosphate esters or GKRPIs and GKAs binding to allosteric sites of GKRP and GK respectively). However, a mechanistic explanation for this phenomenology, potentially of high biological significance, remains to be found.

Further critical experimental material and conceptual commentary on the biochemical characteristics of GK-W99R/W167F/W257F

To facilitate interpretation of our results we characterized GK-W99R/W167F/W257F in greater detail. We have already published [4] the following biochemical characteristics of the tryptophan-free GK reagent (mutant compared with WT enzyme): recombinant protein yield = 19.2 compared with 43.5 mg/l; $k_{cat} = 6.14$ compared with 62.8 1/s; glucose $S_{0.5} = 4.8$ compared with 7.5 mM; H (glucose) = 1.45 compared with 1.77; ATP $K_m = 1.96$ compared with 0.49; and relative activity index $GI = 0.33$ compared with 1.0 as well as normal responsiveness to GKRP inhibition and GKA activation. The 90 % reduction in the k_{cat} value is most noteworthy, yet is probably least significant for the present binding studies. However, the near total glucose dependency of GKA action seen with GK-WT is lost in Trp^{99}-modified GK and is highly relevant (Figure S2 and Tables S2 and S3). Although binding to GK-WT in the absence of glucose was barely detectable, affinity was near maximal at a glucose concentration of 7.5 mM ($K_d = 0.41$ μM; Figure S2). It is remarkable that the affinity of the known Trp^{99} GK mutants (GK-W99C, GK-W99L and GK-W99R) and GK-W99R/W257F

[1] To whom correspondence should be addressed (email matsch@mail.med.upenn.edu).

have highly comparable glucose-independent K_d values for GKA (Table S2). To explore the allosteric site of non-fluorescent GK-W99R/W167F/W257F in greater detail, we introduced an ectopic tryptophan residue at position Thr[65]. The loop spanning residues Val[62] to Gly[72] undergoes a drastic rearrangement during GK activation by sugars or GKA [10,11]. We therefore expected that the TF signal for GK-T65W/W99R/W167F/W257F would allow us to determine the K_d value of this protein for GKA. Ultimately, its affinity for GKA was indeed comparable with that of GK-WT ($K_d = 0.51\ \mu$M; Figure S3). At saturating GKA levels, glucose affinity was increased approximately 6-fold, which is comparable with the degree of activation observed for GK-WT (Figure S3). These data clearly demonstrate that the process of allosteric activation remains intact for GK-T65W/W99R/W167F/W257F (Figures S3 and S4, and Table S3). The observed lowering of the Hill coefficient of GK-W99R/W167F/W257F can be explained by the reduced k_{cat} value of the modified GK [7,8]. Time-dependency experiments allowed us to calculate the activation energy (E_a) of ligand-induced slow conformational transitions for WT and mutant GK proteins (K140E, S263P, M298K, S336L, W99R and W99R/W257F) (Figure S1 and Table S1). Ligand binding resulted in a slow transition from a low to a high sugar affinity conformation of the enzyme, a response classically seen with hysteretic enzymes [5–9]. GKA activation of GK-K140E, GK-S263P, GK-M298K and GK-S336L required the presence of MH, whereas GK-W99R and GK-W99R/W257F (here referred to as the W167 enzyme) responded to GKA alone (Figure S4). The rate constants of GK-W99R and GK-W99R/W257F were highest (Table S1), which seems to indicate that Trp[99] sterically hinders GKA access in the open conformation of the WT enzyme (Figures S9A and S9B). The rate of transition was increased by temperature as indicated by the transition times and rate constants. The calculated E_a value for ligand-induced activation ranged from 48.8 to 73.1 kJ/mol and was practically the same for GK-WT, GK-W99R and GK-W99R/W257F. These data demonstrate that neither Trp[99] substitution nor drastic reengineering of the GK protein compromise the basic process of ligand-induced GK activation. Table S3 shows a range of GKA K_d values for all Trp[99] substitution mutants varying from 0.4 to 0.51 μM, suggesting that the GKA affinity for GK when complexed with GKRP was markedly decreased compared with that of free GK, similar to the effect of complex formation on glucose binding to GK and on F1P binding to GKRP (Tables S1–S4 and Figures S10–S12 and the glucose affinity of 4.8 mM for GK-W99R/W167F/W257F described above). Because of the described quantitative and qualitative impact that the mutational modification exerts on the GK reagent of our assay system we describe and interpret the present experiments as model studies, but conclude that extrapolation to the normal situation are highly meaningful and relevant.

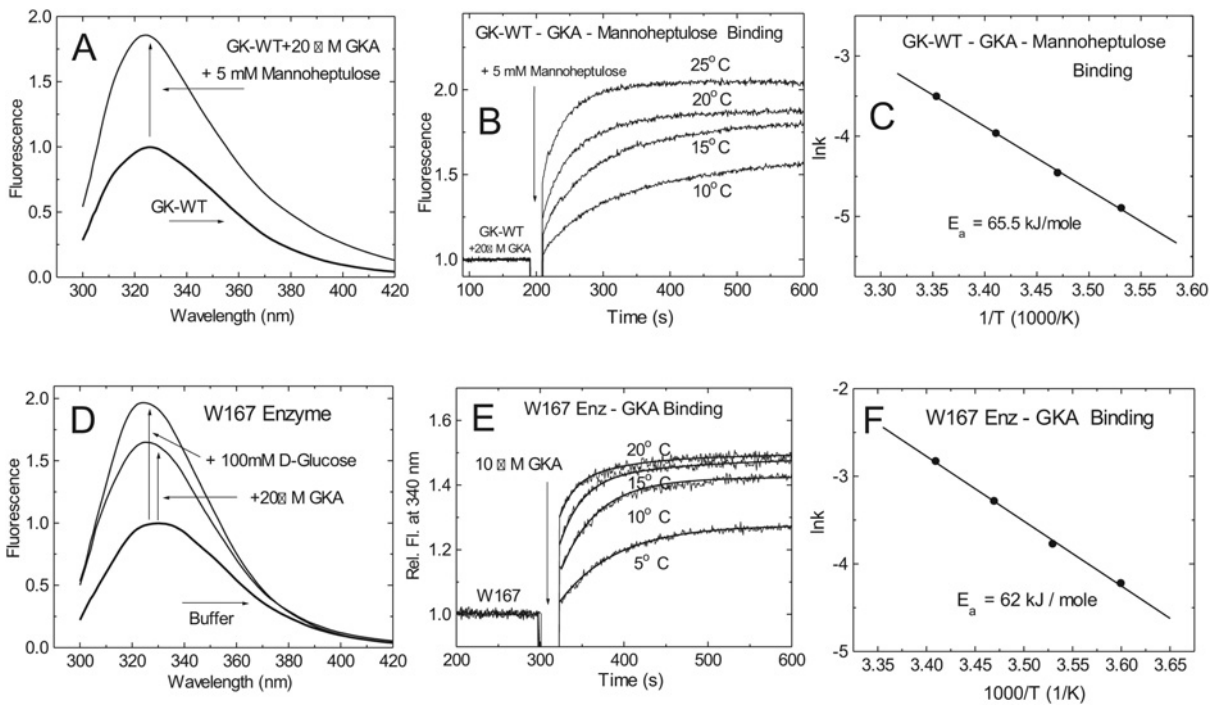

Figure S1 TF measurements illustrating the slow ligand-induced conformational transition of GK-WT and GK-W99R/W257F (W167 enzyme)

(**A**) TF of ~1 μM GK-WT in the presence or absence of 5 mM MH plus 20 μM GKA. Note that the K_d values for MH decreased from 17 mM to 1 mM in the presence of GKA. (**B**) Temperature dependency of the MH/GKA-induced transition process. Binding of GKA requires the presence of both MH and GKA. (**C**) Arrhenius plot of the data in (**B**) allowing for calculation of the activation energy of the transition process. (**D**) TF of the W167 enzyme (i.e. GK-W99R/W257F) in the presence of 20 μM GKA or 100 mM D-glucose. (**E**) Kinetics of the temperature-dependent increase in TF following the addition of 10 μM GKA. For the W167 enzyme, the increase in TF in the presence of GKA is sugar-independent. (**F**) Arrhenius plot of GKA-induced activation of the W167 enzyme. (**A**, **B** and **C**) are modified from [18]: American Diabetes Association, Glucokinase Activators for Diabetes Therapy: May 2010 status report, American Diabetes Association, 2011. Copyright and all rights reserved. Material from this publication has been used with the permission of American Diabetes Association. © 2011, American Diabetes Association.

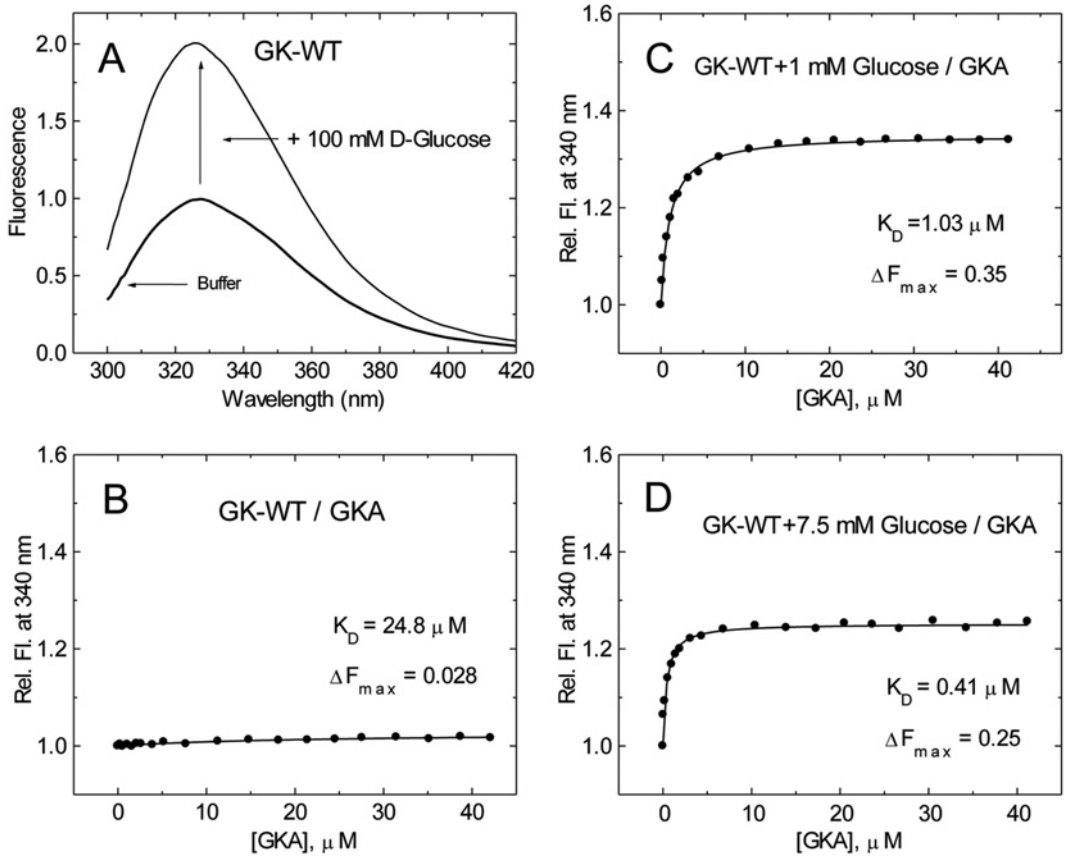

Figure S2 Relative change in TF for 0.9 μM GK-WT at 20°C

In the presence or absence of 100 mM D-glucose (**A**), in the presence of increasing amounts of GKA (**B**), in the presence of 1 mM D-glucose and increasing amounts of GKA (**C**), and in the presence of 7.5 mM D-glucose and increasing amounts of GKA ($\lambda_{exc} = 295$ nm; $\lambda_{em} = 340$ nm).

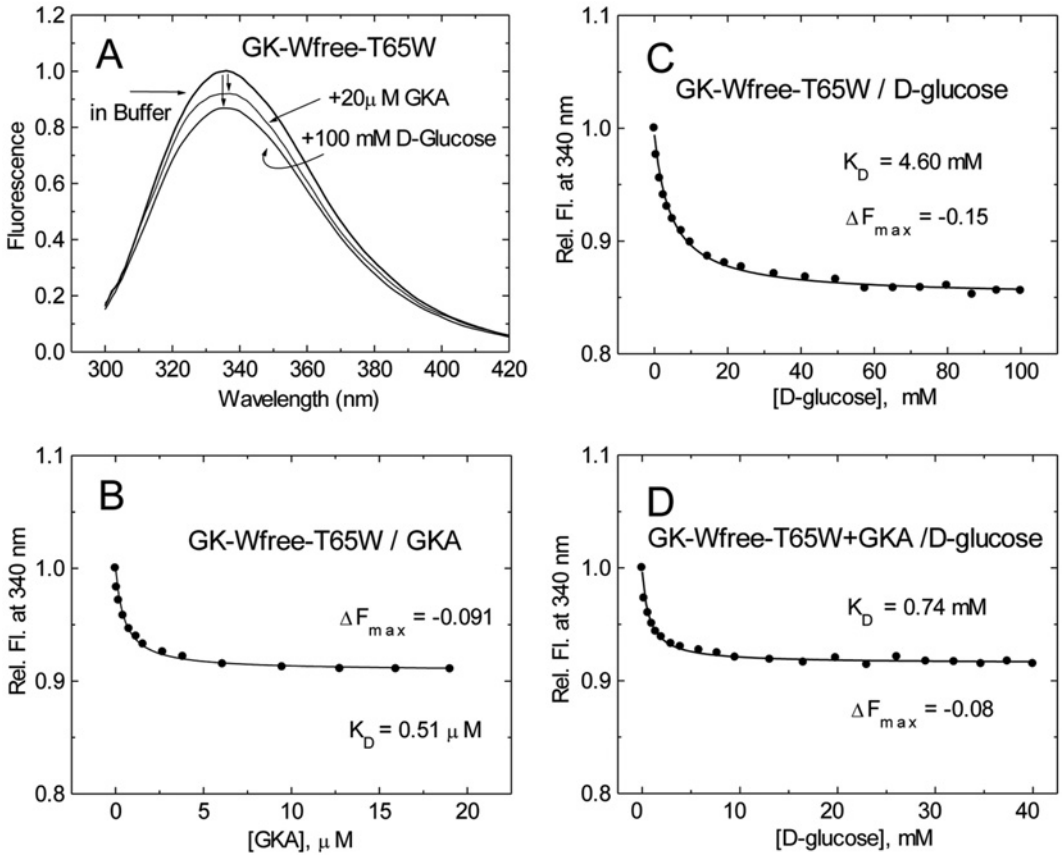

Figure S3 Fluorimetric evidence for glucose binding and glucose-independent GKA binding by GK-T65W/W99R/W167F/W257F at 25°C

(**A**) Decrease in TF in the presence of 20 μM GKA or in the presence of 100 mM D-glucose. (**B**) Effect of increasing amounts of GKA on this decrease. (**C**) Decrease in TF upon titration with D-glucose and (**D**) decrease in TF upon titration with D-glucose in the presence of 20 μM GKA ($\lambda_{exc} = 295$ nm; $\lambda_{em} = 340$ nm).

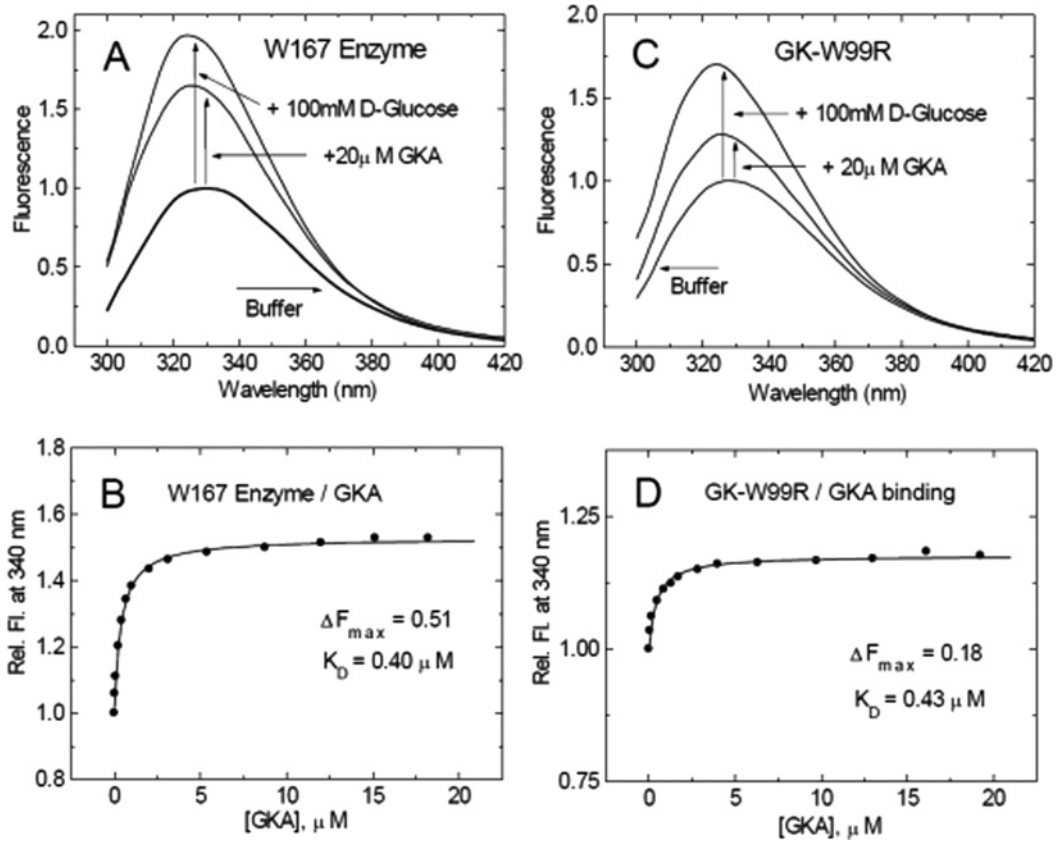

Figure S4 Fluorimetric evidence for glucose-independent GKA binding by the W167 enzyme (i.e. GK-W99R/W257F) and GK-W99R

(**A** and **C**) Increase in the presence of 20 μM GKA or 100 mM D-glucose. (**B** and **D**) Effect of increasing amounts of GKA on this increase ($\lambda_{exc} = 295$ nm; $\lambda_{em} = 340$ nm).

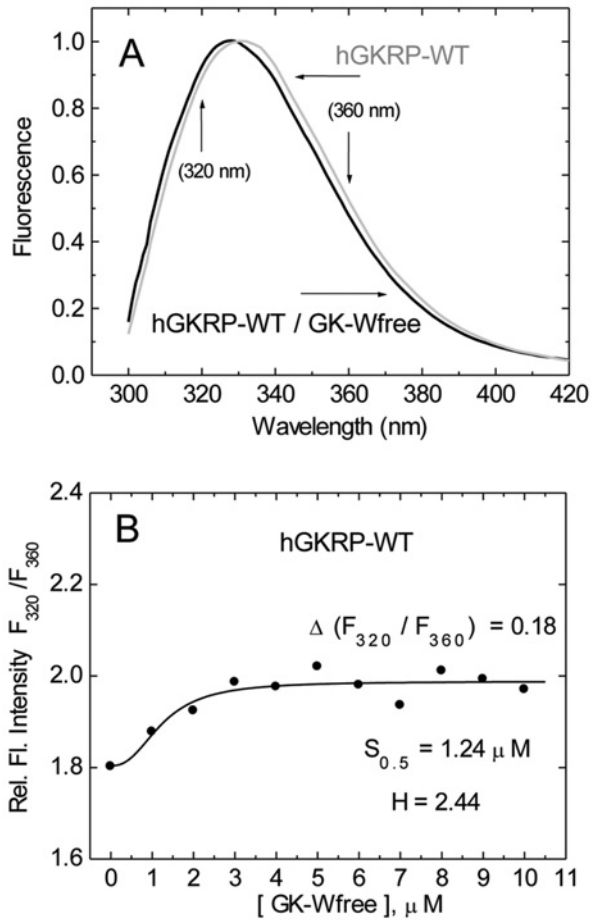

Figure S5 Demonstration of the GK-induced fluorescence blue shift of GKRP

(**A**) Normalized TF spectra for 0.3 μM GKRP-WT showing a 5 nm blue shift in the presence of 5 μM GK-W99R/W167F/W257F ($\lambda_{exc} = 295$ nm). (**B**) Relative fluorescence intensity increase at 320 and 360 nm (F_{320}/F_{360}) as a function of increasing amount of GK-W99R/W167F/W257F.

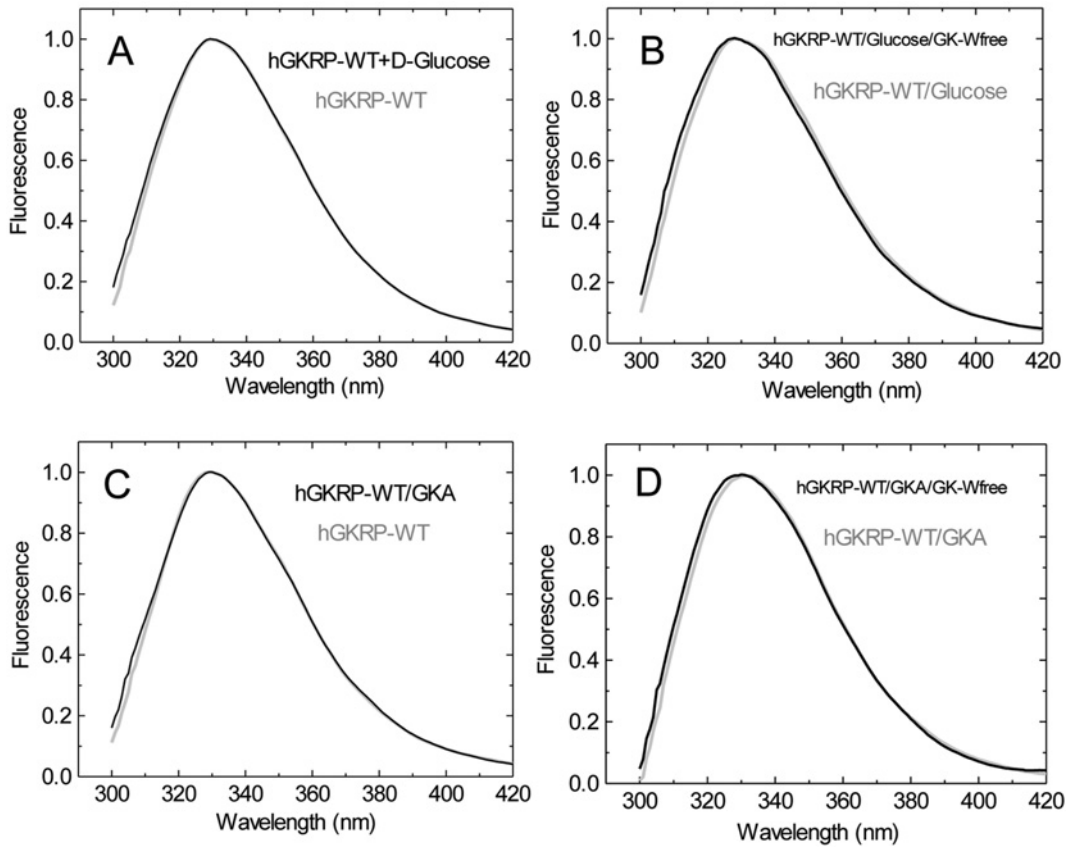

Figure S6 Normalized TF spectra for 0.3 μM GKRP-WT

(**A**) Normalized TF spectra in the presence or absence of 100 mM D-glucose. (**B**) The effect of 5 μM GK-W99R/W167F/W257F on the TF of GKRP-WT in the presence of 100 mM D-glucose. (**C**) Normalized TF spectra in the presence or absence of 20 μM GKA. (**D**) The effect of 5 μM GK-W99R/W167F/W257F on the TF spectrum of GKRP-WT in the presence of 20 μM GKA ($\lambda_{exc} = 295$ nm).

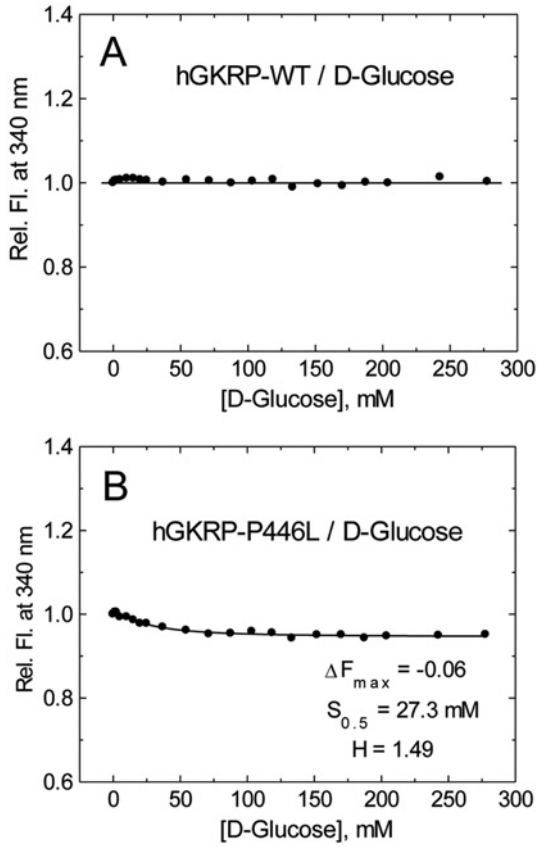

Figure S7 Relative change in TF for 0.3 μM GKRP in the presence of increasing amounts of D-glucose

For GKRP-WT (**A**) and for GKRP-P446L (**B**) ($\lambda_{exc} = 295$ nm; $\lambda_{em} = 340$ nm).

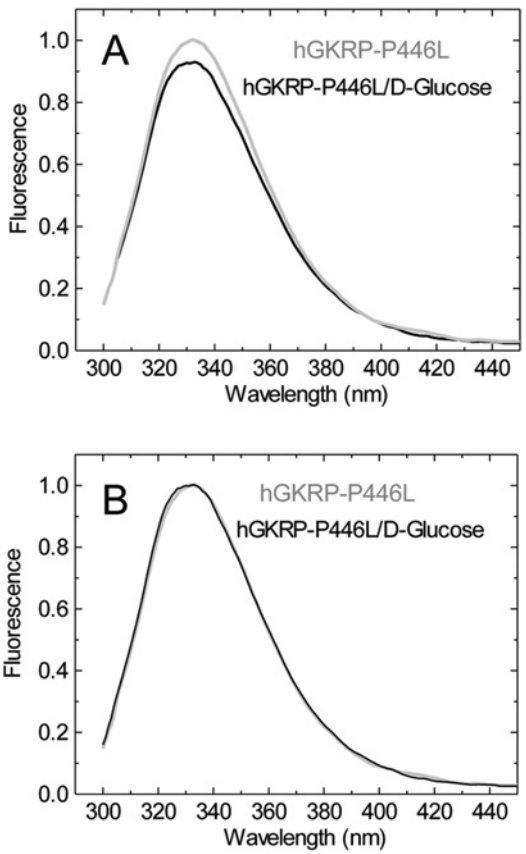

Figure S8 Atypical glucose binding to GKRP-P446L

(**A**) TF spectra for 0.3 μM GKRP-P446L in the presence or absence of 100 mM D-glucose. (**B**) Normalized TF of GKRP-P446L from (**A**).

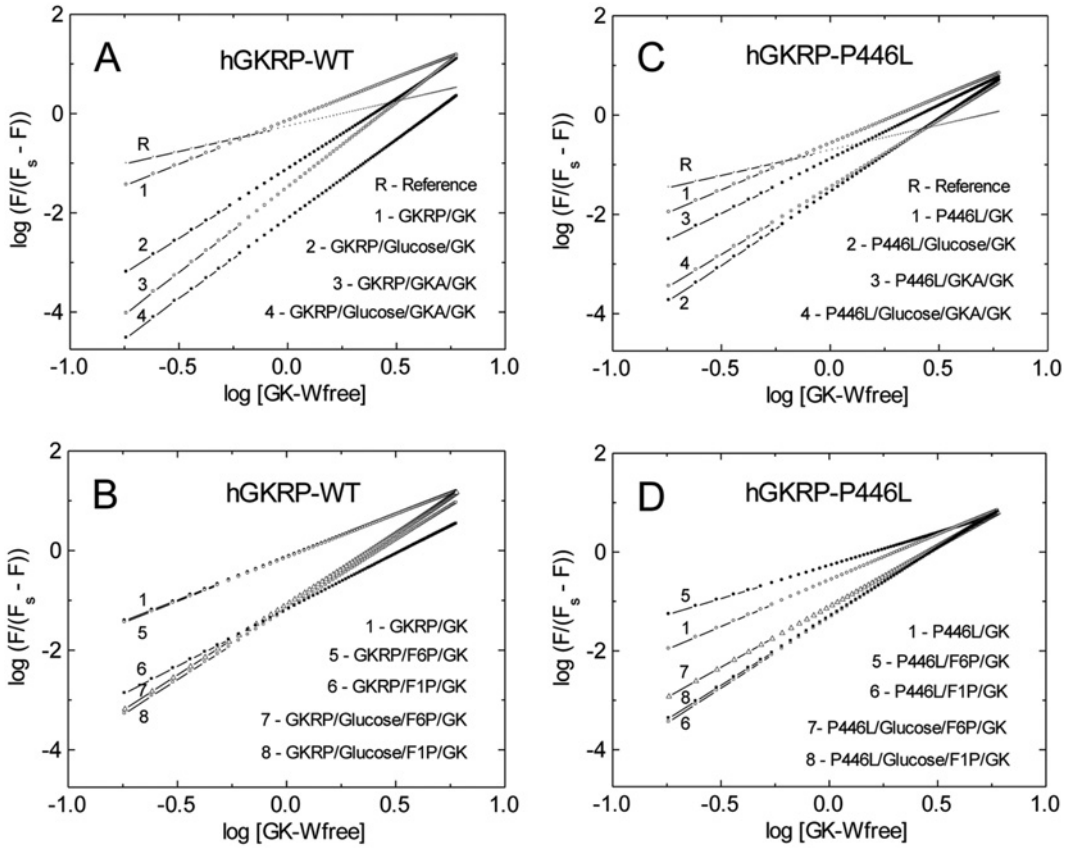

Figure S9 Co-operativity of GK–GKRP complex assembly presented as Hill plots

Hill plots for GK-W99R/W167F/W257F binding to GKRP-WT and GKRP-P446L as measured by TF GKRP fluorescence as a function of glucose and GKA binding (**A** and **C**) and as a function of F6P, F1P and glucose binding as indicated (**B** and **D**). The plots are based on data shown in Figures S6–S8.

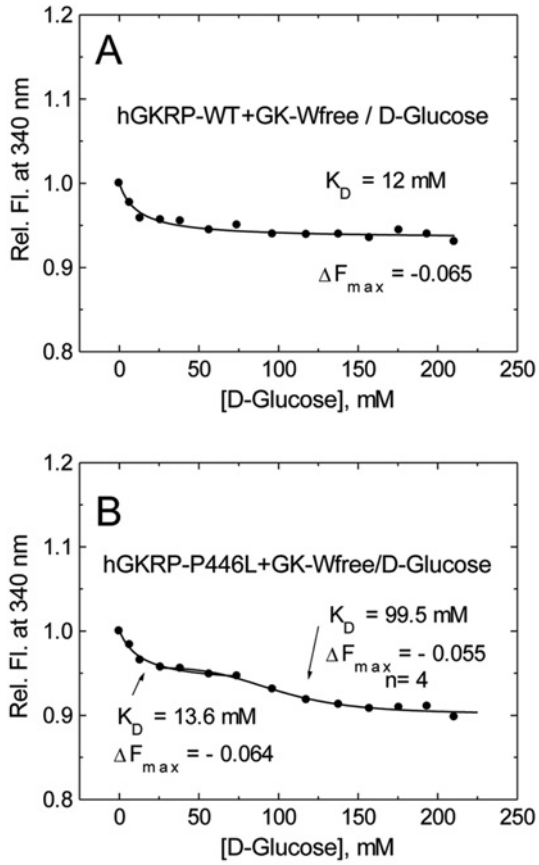

Figure S10 Relative change in TF for 0.3 μM GKRP and 1 μM GK in the presence of increasing amounts of D-glucose

For GKRP-WT (**A**) and GKRP-P446L (**B**) ($\lambda_{exc} = 295$ nm; $\lambda_{em} = 340$ nm). GK-Wfree, GK-W99R/W167F/W257F.

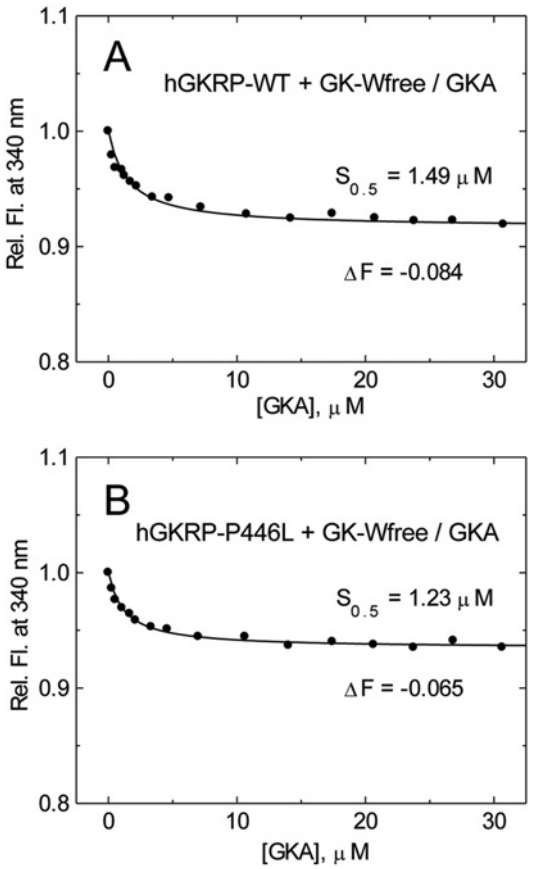

Figure S11 Relative decrease in TF for 0.3 μM GKRP bound to GK (1 μM) in the presence of increasing amounts of GKA

For GKRP-WT (**A**) and for GKRP-P446L (**B**) ($\lambda_{exc} = 295$ nm; $\lambda_{em} = 340$ nm). GK-Wfree, GK-W99R/W167F/W257F.

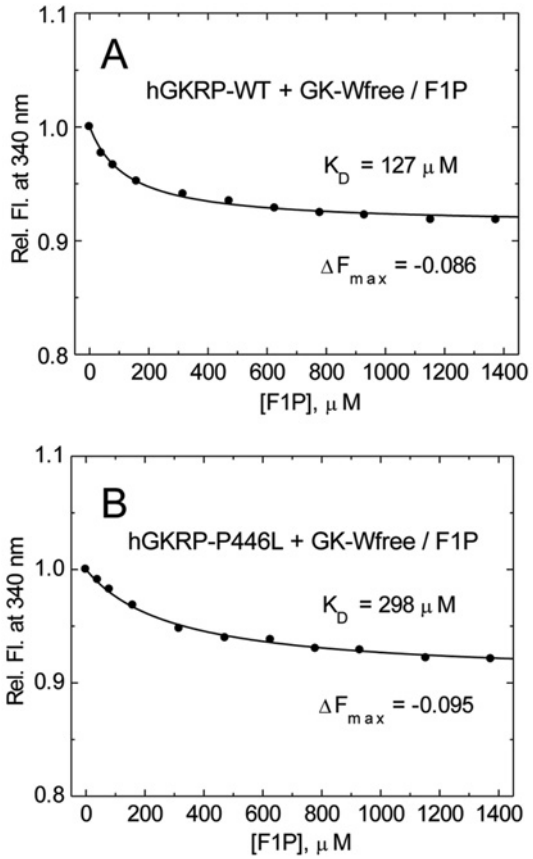

Figure S12 Relative decrease in TF for 0.3 μM GKRP bound to 1 μM GK-W99R/W167F/W257F in the presence of increasing amounts of F1P

For GKRP-WT (**A**) and GKRP-P446L (**B**) ($\lambda_{exc} = 295$ nm; $\lambda_{em} = 340$ nm).

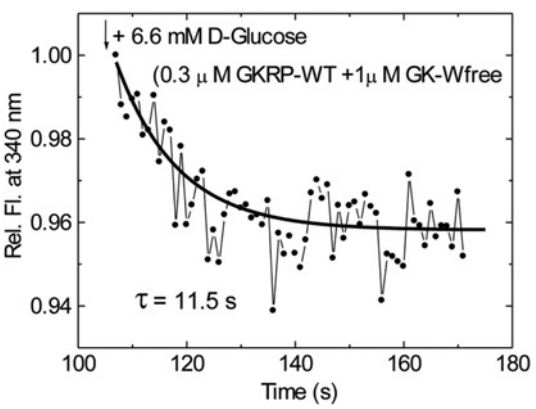

Figure S13 Time-dependent decrease in GKRP-WT TF upon addition of 6.6 mM D-glucose containing 0.3 μM GKRP and 1 μM GK in buffer (pH 7.2)

Data fitted to a mono ExpDecay function yields values of $\tau = 11$ s and $A = 0.04$ ($\lambda_{exc} = 295$ nm; $\lambda_{em} = 340$ nm). GK-Wfree, GK-W99R/W167F/W257F.

Table S1 Temperature dependence of the kinetics for ligand binding to GK-WT and GK mutants measured by TF

Results are the thermodynamic parameters for the activation process.

GK	Ligand(s) (concentration)	Temperature (°C)	Time (s)	k (s^{-1})	ΔE_a (kJ/mol)	$\Delta H°$ (kJ/mol)	$\Delta S°$ (kJ/molK)	$\Delta G°$ (kJ/mol)
GK-WT	GKA (20 μM)/MH (1 mM)	25.0	33.4	2.99×10^{-2}	65.5	63.0	− 62.8	81.7
		20.0	52.9	1.89×10^{-2}				
		15.0	86.6	1.15×10^{-2}				
		10.0	134.4	0.74×10^{-2}				
GK-S336L	GKA (20 μM)/MH (10 mM)	25.4	37	2.70×10^{-2}	48.8	44.3	− 119.5	81.9
		20.1	52.7	1.90×10^{-2}				
		15.0	72.2	1.39×10^{-2}				
		10.1	106.3	0.94×10^{-2}				
GK-M298K	GKA (20 μM)/MH (10 mM)	25.4	34.9	2.87×10^{-2}	60.7	58.2	− 79.2	81.8
		20.1	54.1	1.85×10^{-2}				
		15.0	85.2	1.17×10^{-2}				
		10.1	126.9	0.79×10^{-2}				
GK-S263P	GKA (20 μM)/MH (10 mM)	25.4	32.7	3.06×10^{-2}	53.6	51.1	− 99.9	80.9
		20.1	47.6	2.10×10^{-2}				
		15.0	64.0	1.56×10^{-2}				
		10.1	105.7	0.95×10^{-2}				
GK-K140E	GKA (20 μM)/MH (10 mM)	25.4	20.6	4.85×10^{-2}	73.1	70.6	− 33.7	80.6
		20.1	38.3	2.61×10^{-2}				
		15.0	58.5	1.71×10^{-2}				
		10.1	101.7	0.98×10^{-2}				
GK-W99R	GKA (20 μM)	20.1	11.8	8.48×10^{-2}	60.7	58.2	− 66.8	78.1
		15.0	19.6	5.38×10^{-2}				
		10.1	30.1	3.32×10^{-2}				
		4.6	44.7	2.24×10^{-2}				
GK-W99R/W257F	GKA (20 μM)	20.1	17.0	5.88×10^{-2}	61.5	59.0	− 67.2	79.0
		15.0	26.8	3.73×10^{-2}				
		10.1	43.7	2.29×10^{-2}				
		4.6	68.5	1.46×10^{-2}				

Table S2 GKA binding by GK-WT at 20°C in the absence and presence of D-glucose measured by TF

All reactions used 0.9 μM GK-WT. ΔF is the relative fluorescence change at 340 nm.

D-glucose (mM)	ΔF	K_d (μM)	H	χ^2
None	0.028	25	1	1.0×10^{-5}
1	0.35	1.03	1	4.4×10^{-5}
7.5	0.25	0.41	1	23×10^{-5}

Table S3 Glucose and GKA binding by GK-W99R/W257F, GK-W99R and GK-T65W/W99R/W167F/W257F measured at 20°C by TF of hGKRP and GK mutants

ΔF is the relative fluorescence change at 340 nm.

Combinations of proteins and ligands	ΔF	K_d (μM)	H	χ^2
GK-W99R/W257F	0.51	0.40	1	9.7×10^{-5}
GK-W99R	0.18	0.43	1	5.8×10^{-5}
GK-T65W/W99R/W167F/W257F	− 0.091	0.51	1	1.0×10^{-5}
GK-T65W/W99R/W167F/W257F	− 0.15	4.60*	1	1.2×10^{-5}
GK-T65W/W99R/W167W257F and GKA	− 0.08	0.74*	1	1.0×10^{-5}

*D-glucose binding at 25°C (mM).

Table S4 TF quantum yields ($\Phi \pm 0.02$) of hGKRP-WT and hGKRP-P446L under different medium conditions at 20°C

The buffer contained 20 mM phosphate, 50 mM KCl, 1 mM EDTA and 1 mM DTT (pH 7.2).

Medium	hGKRP-WT Φ Fl. λ_{max}(nm)	hGKRP-P446L Φ Fl. λ_{max}(nm)	Trp-NATA Φ Fl. λ_{max}(nm)
Buffer	0.22 (332)	0.24 (332)	0.14 (350)
Urea (8 M)	0.14 (340)*	0.15 (340)*	–

*n^2 (urea)/n^2 (H_2O) = 1.103.

Table S5 $\Delta G(H_2O)$ value from urea denaturation curves for GK-WT and hGKRP-WT and their mutants in buffer at 20°C

The buffer contained 20 mM phosphate, 50 mM KCl, 1 mM EDTA and 1 mM DTT (pH 7.2).

Protein	$\Delta G(H_2O)$ ($\pm$ 0.05 kcal/mol)
GK-WT	1.63
GK-S263P	1.33
GK-M298K	1.38
GKRP-WT	1.56
hGKRP-P446L	1.55

Table S6 Curve fitting analysis of hGKRP-WT/hGKRP-P446L and GK-W99R/W167F/W257F interactions in the absence and presence of F6P at 20 °C measured by the TF of hGKRP

ΔF is the relative fluorescence change at 340 nm.

Agents	ΔF	$S_{0.5}$ (μM)	H	χ^2
hGKRP-WT and GK-W99R/W167F/W257F	0.29	1.22	1.74	7.4×10^{-5}
	0.39	1.85	1	18×10^{-5}
hGKRP-WT, F6P and GK-W99R/W167F/W257F	0.31	1.20	1.71	1.7×10^{-5}
	0.43	1.84	1	15×10^{-5}
hGKRP-P446L and GK-W99R/W167F/W257F	0.44	2.05	1.86	4.2×10^{-5}
	0.82	5.23	1	28×10^{-5}
hGKRP-P446L , F6P and GK-W99R/W167F/W257F	0.44	1.66	1.31	29×10^{-5}
	0.55	2.45	1	29×10^{-5}

REFERENCES

1 Monod, J., Wyman, J. and Changeux, G. P. (1963) On the nature of allosteric transition: a possible model. J. Mol. Biol. **12**, 88–119

2 Koshland, D. E., Nemethy, G. and Filmer, D. (1966) Comparison of experimental binding data and theoretical models in proteins containing subunits. Biochemistry **5**, 365–385

3 Changeux, G. P. (2011) 50th anniversary of the word "allosteric". Protein Sci. **20**, 1119–1124

4 Zelent, B., Odili, S., Buettger, C., Shiota, C., Grimsby, J., Taub, R., Magnuson, M. A., Vanderkooi, J. M. and Matschinsky, F. M. (2008) Sugar binding to recombinant wild-type and mutant glucokinase monitored by kinetic measurement and tryptophan fluorescence. Biochem. J. **413**, 269–280

5 Neet, K. E. and Ainslie, Jr, G. R. (1980) Hysteretic enzymes. Methods Enzymol. **64**, 192–226

6 Neet, K. E., Keenan, R. P. and Tippett, P. S. (1990) Observation of a kinetic slow transition in monomeric glucokinase. Biochemistry **29**, 770–777

7 Cornish-Bowden, A. (1995) Fundamental Enzyme Kinetics. Portland Press, London

8 Cornish-Bowden, A. and Cardenas, M. L. (2004) Glucokinase: a monomeric enzyme with postitive co-operativity, In Glucokinase and Glycaemic Diseases: From Basics to Novel Therapuetics (Matschinsky, F. and Magnuson, M. A., eds), pp. 125–134, Karger, Basel

9 Frieden, C. (1979) Slow transitions and hysteretic behavior in enzymes. Ann. Rev. Biochem. **48**, 471–489

10 Zelent, B., Odili, S., Buettger, C., Zelent, D. K., Chen, P., Fenner, D., Bass, J., Stanley, C., Laberge, M., Vanderkooi, J. M. et al. (2011) Mutational analysis of allosteric activation and inhibition of glucokinase. Biochem. J. **440**, 203–215

11 Matschinsky, F. M., Zelent, B., Doliba, N. M., Kaestner, K. H., Vanderkooi, J. M., Grimsby, J., Berthel, S. J. and Sarabu, R. (2011) Research and development of glucokinase activators for diabetes therapy: theoretical and practical aspects. Handb. Exp. Pharmacol. **203**, 357–401

12 Szlyk, B., Braun, C. R., Ljubicic, S., Patton, E., Bird, G. H., Osundiji, M. A., Matschinsky, F. M., Walensky, L. D. and Danial, N. N. (2013) A phosphor-BAD BH3 helix activates glucokinase by a mechanism distinct from that of allosteric activators. Nat. Struct. Mol. Biol. **21**, 36–42

13 Choi, J. M., Seo, M. H., Kyeong, H. H., Kim, E. and Kim, H. S. (2013) Molecular basis for the role of glucokinase regulatory protein as the allosteric switch for glucokinase. Proc. Natl. Acad. Sci. U.S.A. **110**, 10171–10176

14 Agius, L. (2008) Glucokinase and molecular aspects of liver glycogen metabolism. Biochem. J. **414**, 1–18

15 Lloyd, D. J., St Jean, Jr, D. J., Kurzeja, R. J. M., Wahl, R. C., Michelsen, K., Cupples, R., Chen, M., Wu, J., Sivits, G., Helmering, J. et al. (2013) Antidiabetic effects of glucokinase regulatory protein small-molecule disruptors. Nature **504**, 437–440

16 Hill, A. V. (1910) The possible effect of aggregation of the molecules of hemoglobin on its dissociation curves. J. Physiol. **40**, 389–403

17 Hill, A. V. (1969) Bayliss and Starling and the happy fellowship of physiologists. J. Physiol. **204**, 1–13

18 Matschinsky, F. M., Zelent, B., Doliba, N., Li, C., Vanderkooi, J. M., Naji, A., Sarabu, R. and Grimsby, J. (2011) Glucokinase activators for diabetes therapy: May 2010 status report. Diabet. Care **34**, S236–S243

Received 11 October 2013/3 February 2014; accepted 26 February 2014
Published as BJ Immediate Publication 26 February 2014, doi:10.1042/BJ20131363